2014 - 2020 Interreg V-A

Italy - Croatia CBC Programme

Call for proposal 2019 Strategic

CoAStal and marine waters integrated monitoring systems for ecosystems proteCtion AnD managemEnt

CASCADE

Project ID: 10255941

Priority Axis: Environment and cultural heritage

Specific objective: Improve the environmental quality conditions of the sea and coastal area by use of sustainable and innovative technologies and approaches

D3.4.1

Report on the model design for marine coastal environment characterization for each Pilot

PP in charge: PP1 – CMCC

Final version

Public document

September, 2021

Project acronym	**CASCADE**
Project ID number	**10255941**
Project title	**CoAStal and marine waters integrated monitoring systems for ecosystems protection AnD managemEnt**
Priority axis	**3 - Environment and cultural heritage**
Specific objective	**3.2 - Contribute to protect and restore biodiversity**
Strategic theme	**3.2.1 - Marine environment**
Word Package number	**WP3**
Word Package title	**Coastal Marine Environment characterization of (species and) ecosystems**
Activity number	**Activity 3.4**
Activity title	**Models design for marine coastal environment characterization**
Partner in charge	**PP1 – CMCC**
Partners involved	**All PPs**

Table of Contents

1. Aims and content of the document

The aim of the Deliverable is to describe the design of the modelling implementation foreseen in the framework of CASCADE WP3 and finalized in terms of modelling simualtion and foreacasting in WP4.

The report follows the different spatial scales covered by CASCADE implementation plan, from the regional (e.g. Mediterranean Sea, Adriatic Sea) to pilot scale (e.g. very local implementations). Accordingly, the report is organized as follows. Section 2 introduces the regional scale with the description of (i) the Mediterranena Sea CMEMS (https://marine.copernicus.eu/) hydrodynamic modelling system and (ii) the new high-resolution coastal modelling system for the Adriatic Sea developed in CASCADE. Section 3 presents the selected pilot sites in the Croatian and Italian marine hotspot coastal areas.

2. Regional scale modelling

2.1. Med-CMEMS hydrodynamic modelling system

The CMEMS (Copernicus Marine Environment Monitoring Service) Mediterranean Near Real Time System, MedFS, provides analysis and short-term forecast of the main physical parameters in the Mediterranean Sea and it is the physical component of the Med-MFC called Med-Currents. The system is composed of a coupled hydrodynamic-wave model with data assimilation implemented over the whole Mediterranean basin and extended into the Atlantic Sea in order to better resolve the exchanges with the Atlantic Ocean at the Strait of Gibraltar. The model horizontal grid resolution is 1/24˚ (ca. 4.5 km) and has 141 unevenly spaced vertical levels. The MedFS dataset can be freely downloaded from the CMEMS catalogue (Product MEDSEA_ANALYSISFORECAST_PHY_006_013, Clementi et al., 2021). Figure 1 shows the CMEMS MedFS domani and bathymetry.

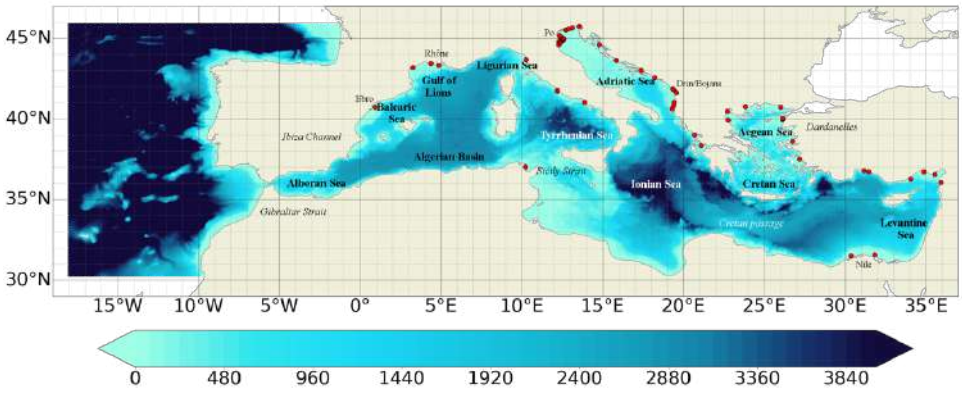

Figure 1. CMEMS MedFS domain and bathymetry

Hydrodynamic model component (NEMO)

The MedFS oceanic equations of motion are solved by an Ocean General Circulation Model (OGCM) based on NEMO (Nucleus for European Modelling of the Ocean) version 3.6 (Madec et al., 2016). The code is developed and maintained by the NEMO-consortium. NEMO has been implemented in the Mediterranean Sea at 1/24° x 1/24° horizontal resolution and 141 unevenly spaced vertical levels (Clementi et al., 2017a) with baroclinic time step of 120 s. The model covers the whole Mediterranean Sea and also extends into the Atlantic in order to better resolve the exchanges with the Atlantic Ocean at the Strait of Gibraltar. The topography is created starting from the GEBCO 30arc-second grid (http://www.gebco.net/data_and_products/gridded_bathymetry_data/gebco_30_second_grid/), filtered (using a Shapiro filter) and manually modified in critical areas such as: islands along the Eastern Adriatic coasts, Gibraltar and Messina straits, Atlantic box edge.

NEMO model solves primitive equations using a time-splitting technique with non-linear free surface formulation and time-varying vertical z-star coordinates. The advection scheme for active tracers, temperature and salinity, is a mixed up-stream/MUSCL (more details in Oddo et al. 2009). The vertical diffusion and viscosity terms are a function of the Richardson number as parameterized by Pacanowsky and Philander (1981). The model interactively computes air-surface fluxes of momentum, mass, and heat. The bulk formulae implemented are described in Pettenuzzo et al. (2010) and are currently used in the Mediterranean operational system (Tonani et al., 2015). A detailed description of other specific features of the model implementation can be found in Oddo et al., (2009, 2014). The vertical background viscosity and diffusivity values are set to 1.2e-6 [m^2/s] and 1.0e-7 [m^2/s] respectively, while the horizontal bilaplacian eddy diffusivity and viscosity are set respectively equal to -1.2e8 [m^4/s] and -2.0e8 [m^4/s].

Tidal waves have been recently (May 2021) included in the system, so that the tidal potential is calculated across the domain for the 8 major constituents of the Mediterranean Sea: M2, S2, N2, K2, K1, O1, P1, Q1. In addition, tidal forcing is applied along the lateral boundaries in the Atlantic Ocean by means of tidal elevation estimated using FES2014 (Carrere et al., 2016) tidal model and tidal currents evaluated using TUGO (Toulouse Unstructured Grid Ocean model, ex-Mog2D, Lynch and Gray 1979).

The hydrodynamic model is nested in the Atlantic within the CMEMS Global analysis and forecast system GLO-MFC daily data set (1/12° horizontal resolution, 50 vertical levels) that is interpolated onto the Med-Currents model grid. Details on the nesting technique and major impacts on the model results are in Oddo et al., (2009). The Dardanelles Strait is also implemented as a lateral open boundary condition by using CMEMS GLO-MFC daily Analysis and Forecast product and daily climatology derived from a Marmara Sea box model (Maderich et al., 2015).

The model is forced by momentum, water and heat fluxes interactively computed by bulk formulae using the 1/10° horizontal-resolution operational analysis and forecast fields from the European Centre for Medium-Range Weather Forecasts (ECMWF) at highest available time frequency (1 hour for

the first 3 days of forecast, 3 hours for the following 3 days of forecast and 6 hours for the last 4 days of forecast and for the analysis) and the model sea surface temperature (details of the air-sea physics are in Tonani et al., 2008). The water balance is computed as Evaporation minus Precipitation and Runoff. The evaporation is derived from the latent heat flux, precipitation is provided by ECMWF as daily averages, while the runoff of the 39 rivers implemented is provided by monthly mean datasets. Objective Analyses-Sea Surface Temperature (OA-SST) fields from CNR-ISA SST-TAC are used for the correction of surface heat fluxes with the relaxation constant of 110 $Wm^{-2}K^{-1}$ centered at midnight since the observed dataset corresponds to the foundation SST (~SST at midnight).

The scientific validation of the modelling system is provided in the Product Quality Information document (https://catalogue.marine.copernicus.eu/documents/QUID/CMEMS-MED-QUID-006-013.pdf). Figure 2 provides as an example a tidal sea level validation in terms of model comparison with respect to tide gauges measurements for M2 and K1 tidal amplitude and phase, showing the ability of the model to accurately represent the tidal elevation.

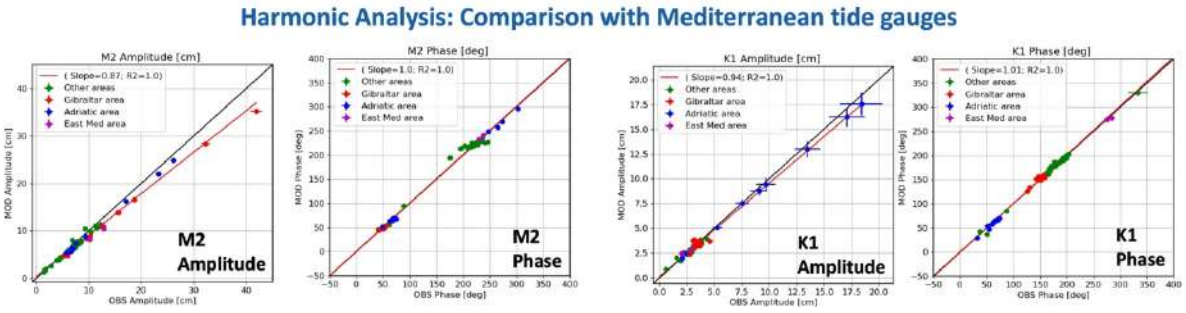

Figure 2. Scatter plots: Model M2 and K1 tidal amplitude and phase with respect to tide gauges measurements.

Wave model component (WW3)

The wave dynamic is solved by a Mediterranean implementation of the WaveWatch-III (WW3) code version 3.14 (Tolman, 2009). WaveWatch covers the same domain and follows the same horizontal discretization of the circulation model (1/24° x 1/24°) with a time step of 240 sec. The wave model uses 24 directional bins (15° directional resolution) and 30 frequency bins (ranging between 0.05 Hz and 0.7931 Hz) to represent the wave spectral distribution.

WW3 has been forced by the same 1/10° horizontal resolution ECMWF atmospheric forcing (the same used to force the hydrodynamic model). The wind speed is then modified by considering a stability parameter depending on the air-sea temperature difference according to Tolman (2002).

The wave model takes into consideration the surface currents for wave refraction but assumes no interactions with the ocean bottom. In the present application WW3 has been implemented following WAM cycle4 model physics (Gunther et al., 1993). Wind input and dissipation terms are based on Janssen's quasi-linear theory of wind-wave generation (Janssen, 1989, 1991). The dissipation term is based on Hasselmann (1974) whitecapping theory according to Komen et al. (1984). The non-linear

wave-wave interaction is modelled using the Discrete Interaction Approximation (DIA, Hasselmann et al., 1985).

Model coupling (NEMO-WW3)

The coupling between the hydrodynamic model (NEMO) and the wave model (WW3) is achieved by an online hourly two-way coupling and consists in exchanging the following fields: NEMO sends to WW3 the air-sea temperature difference and the surface currents, while WW3 sends to NEMO the neutral drag coefficient used to evaluate the surface wind stress. More details on the model coupling and on the impact of coupled system on both wave and circulation fields can be found in Clementi et al. (2017b).

Data assimilation scheme (OceanVar)

The data assimilation system is based on a 3D variational ocean data assimilation scheme, OceanVar, developed by Dobricic and Pinardi (2008) and later upgraded by Storto et al. (2015). The background error covariance matrices vary monthly at each grid point in the discretized domain of the Mediterranean Sea. The observations that are assimilated are derived from CMEMS products: along-track sea level anomaly (a satellite product including dynamical atmospheric correction and ocean tides is chosen) and in-situ vertical temperature and salinity profiles from VOS XBTs (Voluntary Observing Ship-eXpandable Bathythermograph) and ARGO floats.

2.2. High resolution coastal modelling for Adriatic Sea

The coastal modelling system implemented in CASCADE for the entire Adriatic Sea is based on the SHYFEM model, which is a 3-D finite element hydrodynamic model (Umgiesser et al., 2004) solving the Navier–Stokes equations by applying hydrostatic and Boussinesq approximations. The unstructured grid is Arakawa B with triangular meshes (Bellafiore and Umgiesser, 2010; Ferrarin et al., 2013), which provides an accurate description of irregular coastal boundaries. The scalars are computed at grid nodes, whereas velocity vectors are calculated at the centre of each element. Vertically a z layer discretization is applied and most variables are computed in the centre of each layer, whereas stress terms and vertical velocities are solved at the layer interfaces (Bellafiore and Umgiesser, 2010). The peculiarity of unstructured meshes is the ability of representing several scales in a seamless fashion, reaching higher resolution where necessary. The model uses a semi-implicit algorithm for integration over time, which has the advantage of being unconditionally stable with respect to gravity waves, bottom friction and Coriolis terms, and allows transport variables to be solved explicitly. The Coriolis term and pressure gradient in the momentum equation, and the divergence terms in the continuity equation are treated semi-implicitly. Bottom friction and vertical eddy viscosity are treated fully implicitly for stability reasons, while the remaining terms (advective and horizontal diffusion terms in the momentum equation) are treated explicitly. A more detailed description of the model equations and of the discretization method is given in

Umgiesser et al. (2004) and Ferrarin et al. (2017). The model has been already applied to simulate hydrodynamics of several systems in many regions of world, proving its quality and accuracy. Exploiting the variable mesh approach, the model has been successfully applied to several scales, from the open sea (e.g. Mediterranean Sea, Black Sea, Gulf of Mexico) to the coastal seas and estuaries (e.g. coastal areas of Adriatic Ionian and Western Mediterranean Seas in Italy, Kotor Bay in Montenegro, Danube Delta in Romania) to open-sea islands (e.g. Malta) to the fjords (e.g. Roskilde, Denmark, Oslo) to the lagoons (e.g. Venice, Menor in Spain, Nador in Morocco, Dalyan in Turkey, Curonian in Lithuania, Tam Giang in Vietnam) to the ports (e.g. Apulian ports in Italy) to the rivers (e.g. Po river in Italy, Savannah river in Georgia, US) to the lakes (e.g. Geneva in Switzerland, Garda in Italy).

The modelling approach is based on the downscaling of CMEMS Marine products released at the regional scale of Mediterranean Sea (see § 2.1). The current Med-CMEMS implementation is based on NEMO (Nucleus for European Modelling of the Ocean, Madec (2008)) finite-difference code with a horizontal resolution of 1/24 of a degree (4–5 km approximately) and 141 unevenly spaced vertical levels. The system is provided by a data assimilation system based on the 3D-VAR scheme developed by Dobricic and Pinardi (2008).

The area covered by the model unstructured-grid is the Adriatic Sea from 12 to 21°E and 39 to 45.8°N with a horizontal resolution ranging from 2.5km in open sea to 300m at overall coasts. Figure 3 shows the geographical domain, the bathymetry and the overlapped grid. In Figure 4 some enlarged views of the grid in four different coastal hotspots are reported.

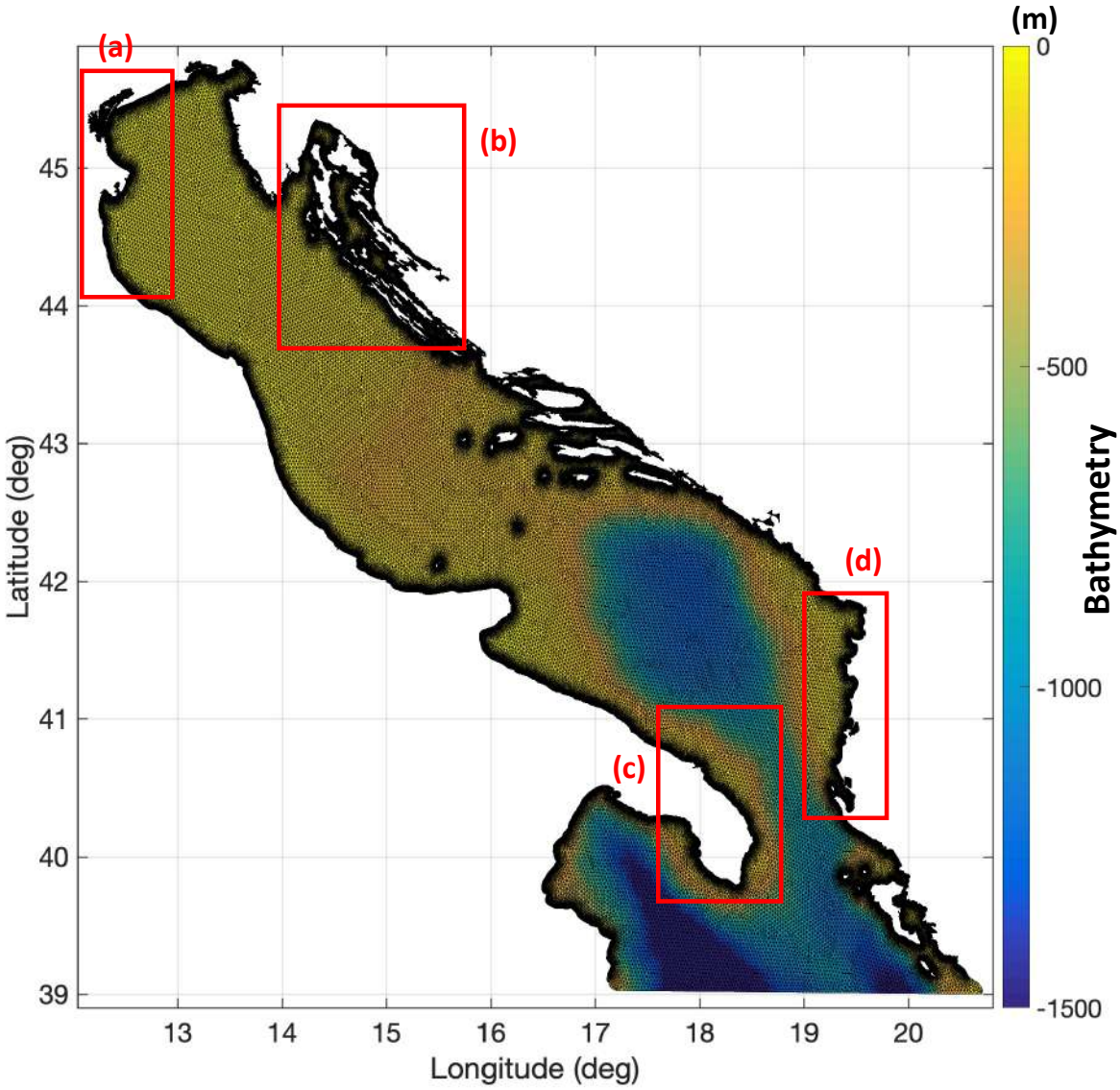

Figure 3: Geographical domain, bathymetry and grid of high resolution coastal modelling for Adriatic Sea

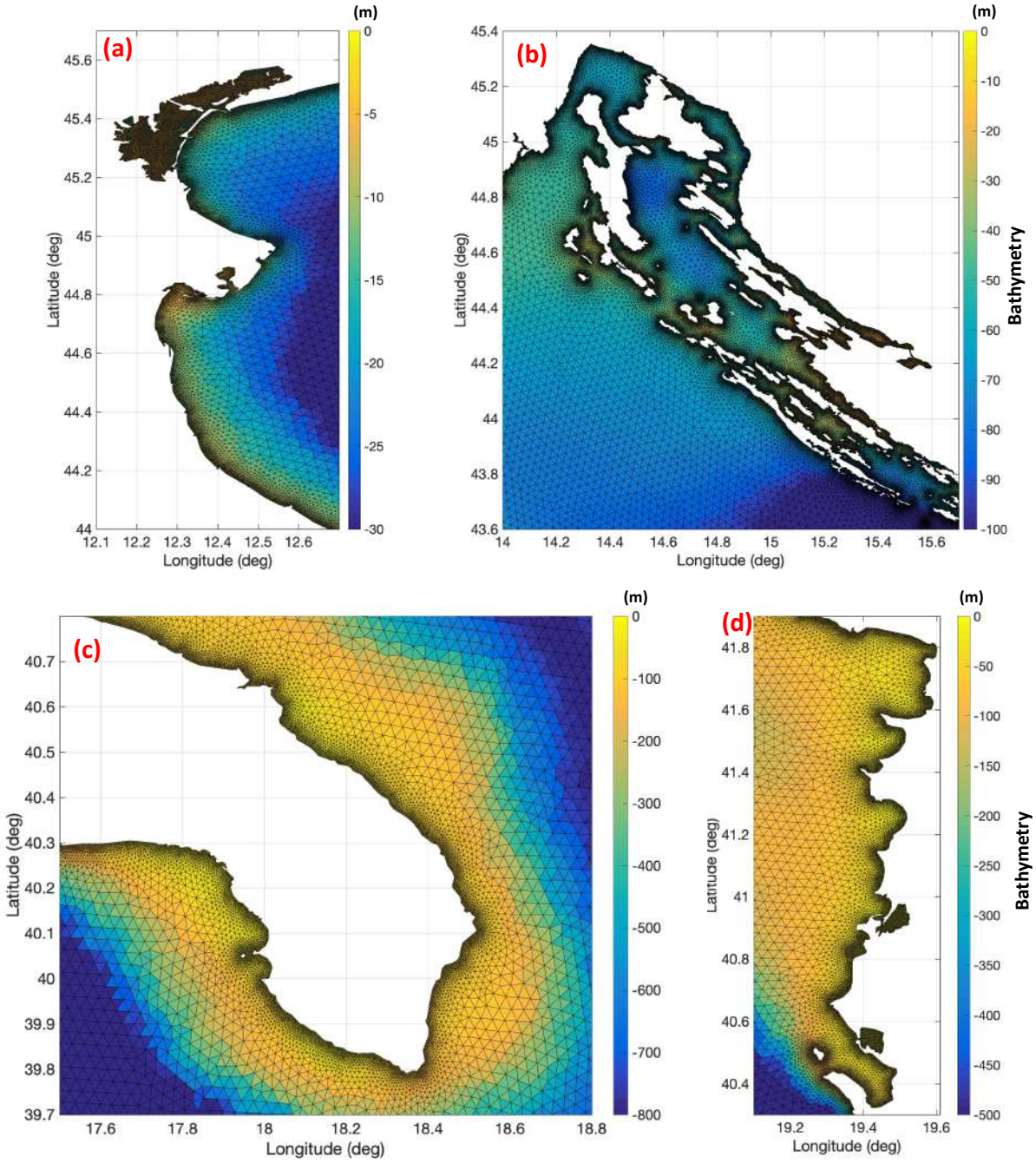

Figure 4: Enlarged views (bathymetry and grid) in coastal zones of high resolution coastal modelling for Adriatic Sea

The bathymetric data used is EMODNET (https://www.emodnet-bathymetry.eu/) product at resolution of 1/16 x 1/16 arc-minutes (circa 110 x 110 meter) resolution. The vertical discretization is based on z-layers approach with 99 levels. The layer thickness is 1m from surface to 20m, then we have 2m of thickness up to 90 meters, then the vertical spacing is progressively (stepwise) increased down to the bottom with a maximum layer thickness of 200 m. This is appropriate for solving the field both in coastal and open-sea areas (Federico et al., 2017).

The modelling systems are three-dimensionally downscaled from Med-CMEMS both in terms or initialization and open boundaries. Clamped type open boundary conditions were employed at the boundary for sea level and inflow active tracers. Total velocities were nudged at the open boundaries and zero gradient boundary conditions were used for outflow active tracers.

The sea level at boundary is imposed combining the non-tidal sea surface height from Med-CMEMS to tidal elevation derived from the OTPS (Oregon State University Tidal Prediction Software (Egbert and Erofeeva, 2002)) tidal model with 1/30 horizontal resolution. Eight of the most significant constituents are considered for astronomical tidal model: M2, S2, N2, K2, K1, O1, P1, Q1.

The basic surface boundary conditions are:

a) For temperature, the air-sea heat flux is parameterized by bulk formulas described in Pettenuzzo et al. (2010), computing Net Long wave radiation (Bignami et al., 1995), Sensible heat (Kondo, 1975), Latent heat (Kondo, 1975), Evaporation (Kondo, 1975), Short Wave Solar Radiation (Reed , 1977), Solar Penetration (Jerlov, 1975).
b) For momentum, surface stress is computed with the wind drag coefficient according to Hellermann and Rosenstein (1983).

For the atmospheric fields, well-consolidated analysis products from ECMWF (~10km resolution and 6h frequency) are adopted as forcing. The atmospheric fields are corrected by land-contaminated points following Kara et al. (2007) and horizontally interpolated at each ocean grid node by means of Cressman's interpolation technique (Cressman, 1959). The atmospheric variables used for the parametrization are 2 m air temperature (T2M), 2 m dew point temperature (D2M), total cloud cover (TCC), mean sea level atmospheric pressure (MSL), and meridional and zonal 10 m wind components (U10M and V10M) and total precipitation (TP).

The release of 62 Adriatic and Ionian rivers in total, 53 flowing into the Adriatic Sea and 9 into the Ionian Sea, has been implemented into model domain (for the dataset refers to Verri et al., 2018). Rivers inputs are treated as clamped boundary condition imposing the discharge, salinity and temperature. Due to a lack of available observations, river inflow surface salinity is fixed to a constant value of 15psu at the river boundaries, except 17 psu for the Po river. These constant salinity values are the result of sensitivity tests performed on the basis of salinity profiles measured at river mouths (Simoncelli et al. 2011) and at the center of the basin (Oddo

et al. 2005). Water temperature at the river adapts to the environmental inner value inside the basin (zero-gradient boundary conditions). For all rivers except Po river, monthly climatologies of discharge are imposed. The monthly discharges have been interpolated on daily basis according to the Killworth (1996) procedure. The Po river discharge consists of daily averages based on observations recorded at Pontelagoscuro station with 30minute frequency (around 40km usptream of the delta mouths). The Po river discharge is unequally subdivided between the nine grid points representing the nine branches of the delta (Po di Goro, Po di Gnocca, Po di Tolle, Po di Bastimento, Po di Scirocco, Po di Bonifazi, Po di Dritta, Po di Tramontana, Po di Maistra) according to percentages in Provini et al. (1992).

About the main numerical settings, in the transport and diffusion equation for scalars we use an average gradient of upwind node scheme for horizontal advection and a TVD (total variation diminishing) scheme for the vertical advection. Horizontal advection of momentum is discretized by an upwind scheme and horizontal eddy viscosity is computed by the Smagorinsky's formulation. For the computation of the vertical viscosities and diffusivities, a k–ε turbulence scheme is used, adapted from the GOTM (General Ocean Turbulence Model) model described in Burchard et al. (1999). The bottom drag coefficient is computed using a logarithmic formulation via bottom roughness length, set homogeneous over the whole system to a value of 0.01 m (Ferrarin et al. 2017).

In this stage of model design we have performed a simulation of 1 year (2018). In Figure 5 we report the seasonal-average circulation fields at 30m for the basin-scale, showing the main structures and dynamics of Adriatic Sea. Next steps will foreseen: (i) longer simulation (up to 3-4 years, i.e. 2018-2020/2021); (ii) validation against different observing datasets (satellite SST, ARGO floats, tidegauges); (iii) short-term operational forecasts. These results will be achieved in deliverable D4.2.1 (Models simulations and forecasting systems).

Thanks to the high resolution at overall coastal scale, the model outputs of the Adriatic Sea system will be also exploited by the Pilots for which specific numerical modeling is not provided in the project.

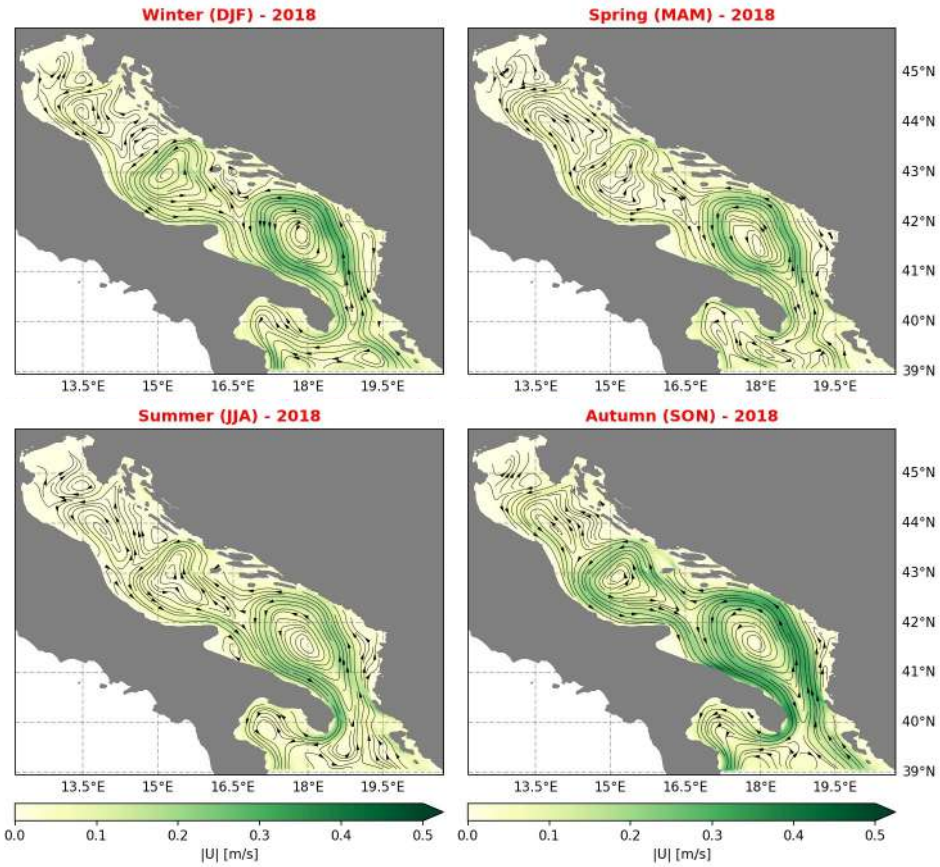

Figure 5: Seasonal-average basin-scale circulation at 30m of high resolution coastal modelling for Adriatic Sea

3. Modelling at the Pilot scale

3.1. Grado and Marano Lagoon, and Gulf of Trieste (IT)

To design the modeling system that will support the characterization and the monitoring of the pilot area, an integrated approach has been adopted. In addition to the model outputs which are available with low spatial resolution at the regional scale, that is the Adriatic basin scale, the high resolution simulations are going to fill in the voids of the coarse outputs, at the pilot scale, in the coastal and lagoon areas. In some parts of the pilot area, the two modeling systems overlap, giving the opportunity to compare the model outputs besides reducing the risk of missing information, especially in the short term forecasting mode, that is foreseen in the activity 4.2 of the project.

The basin scale modelling system is the Copernicus Marine Environment Monitoring Service Mediterranean Near Real Time System, MedFS, (CMEMS), hydrodynamic modelling system, that has

been already described in detail above. The CMEMS 1/24° x 1/24° horizontal resolution model outputs are going to give the boundary conditions for the high resolution modeling code, both in forecast and in hindcast runs. In addition, over the Gulf of Trieste where the coarse grid of CMEMS products is defined, the physical fields of the basin scale model are used as supplemental information and backup for high resolution possible failures.

The high-resolution modeling system, that covers the whole Friuli Venezia Giulia pilot area, is a dynamic downscaling and will be performed with the SHYFEM finite element hydrodynamic model.

The model has been already applied to simulate hydrodynamics in the Mediterranean Sea (Ferrarin et al., 2018), in the Adriatic Sea (Bellafiore et al., 2018), and in several coastal systems (see Umgiesser et al., 2014 and references therein). The good performance of the SHYFEM model in simulating water levels, currents, salinity, and water temperature in the Marano-Grado lagoon and the FVG coast was demonstrated by Ferrarin et al. (2010, 2016).

The numerical computation is going to be performed on a spatial domain that represents part of the northern Adriatic Sea and the lagoon of Marano-Grado by means of the unstructured grid shown in Figure 6. The grid fully contains the Pilot area, see Figure 7. To adequately resolve the river-sea continuum, the unstructured grid also includes the lower part of the other major rivers flowing into the considered system. The use of elements of variable sizes, typical of finite element methods, is fully exploited, in order to suit the complicated geometry of the basin, the rapidly varying topographic features, and the complex bathymetry of the lagoon systems. The numerical grid consists of 33,100 triangular elements with a resolution that varies from 4 km in the open-sea, which is comparable with CMEMS simulations, to a few hundred meters along the coast and tens of meters in the inner lagoon channels. The bathymetry of the northern Adriatic Sea and the Marano-Grado lagoon was obtained by merging several datasets, having different spatial resolution and obtained using different measurement approaches (Madricardo et al., 2017).

The boundary conditions for stress terms (wind stress and bottom drag) follow the classic quadratic parameterization. Heat fluxes are computed at the water surface. Water fluxes between air and sea consist of the precipitation and runoff minus evaporation computed by the SHYFEM model. Smagorinsky's formulation (1963) is used to parameterize the horizontal eddy viscosity. For the computation of the vertical viscosities, a turbulence closure scheme was used. This scheme is adapted from the k-ε module of GOTM (General Ocean Turbulence Model) described by Burchard and Petersen (1999).

The atmospheric forcing for the hydrodynamic model is generated by Weather Research and Forecasting model (WRF ARPA FVG) which is implemented and running operationally at ARPA FVG. Radiation, latent and sensible heat fluxes, besides precipitation, evaporation, temperature and air pressure, both for hindcast (WRF ARPA FVG Hindcast) and forecast (WRF ARPA FVG Forecats) SHYFEM runs are available and ready for use on the hourly base at 2 km x 2 km spatial resolution.

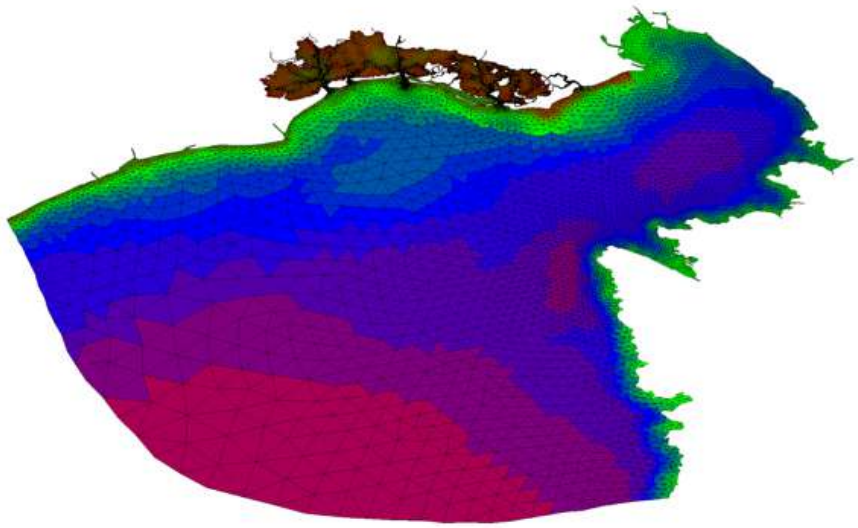

Figure 6: Unstructured grid of the SHYFEM model application to the FVG pilot site.

Figure 7: The Gulf of Trieste area.

From Civil Protection of Friuli-Venezia Giulia region datasets, time series of rivers' discharges for the two main rivers, which are essential for simulations, namely Isonzo and Tagliamento, are available for hindcast runs. Specifically, these data consist in the best integration between measurements and a hydrological numerical model, which is run at the Regional Civil Protection Department of Friuli-Venezia Giulia region. In forecast mode the river outflows are going to be simulated using the WRF model precipitation fields, according to a simple hydrologic model. Concerning the fresh water inflow in the Marano and Grado Lagoon, climatological values are going to be used for hindcasts, while climatological time series will be modulated with forecasted precipitations.

In designing the high resolution modeling system, it was necessary to check its computational compatibility with project resources, to achieve an optimal configuration of software and hardware.

To this end, scalability tests of SHYFEM have been performed on a specific computational node (24 CPUs) of CASCADE projects computational environment, in order to profile and check the performance of the model code. SHYFEM code, 7.5.70 - 2020-12-18 version, has been installed and compiled using the INTEL 19.1 (2020) compiler suite. Shared memory parallel computation (OpenMP, or OMP) has been enabled, while distributed memory parallel computation (Open MPI) is not considered.

The tests refer to simulations performed on the whole Pilot area using boundary conditions for the 2020 August month. Specifically, this benchmark is characterized by the following main features:

- 18311 grid nodes;
- 33100 grid elements;
- 22 model levels;
- 2831 iterations (time steps). One-day simulation

A summary of compoutational times, as a function of used cores, is presented in Figure 8.

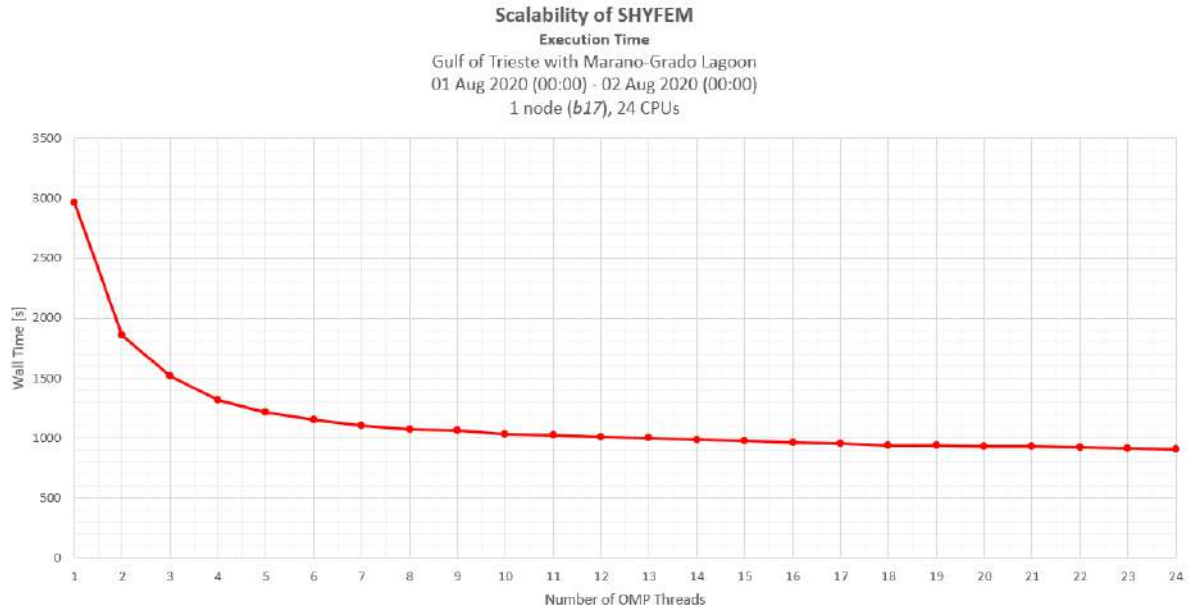

Figure 8: Wall time (seconds) as a function of the number of OpenMP (OMP) threads; scalability test (one-day simulation) of SHYFEM, performed on a specific entire node (b17, 24 CPUs) of C3HPC environment.

According to the scalability results, the high-resolution simulations will be carried on using at most 10 OMP threads because there is no gain in running the code on more resources. Looking at the wall time taken by a full day simulation, it is easy to conclude that the highresolution forecasting modelling system is going to require about one hour and half for a 5-day forecast, while for one year hindcast

run, 120 hours will be needed, including the spin up time necessary to let the code to complete the transient initial phase.

Concerning the data availability for hindcast runs and their validation, a careful evaluation of ARPA FVG datasets, which measurements have been collected through the ordinary institutional and specific monitoring campaigns, the model validation can be performed over a complete year. The choice of the hindcast year will follow, anyway it is worth to be considered falling across year 2017 and the spring of 2019. In Table 1, a summary description of the forcing, boundary conditions and validation measurements, available for the Pilot Area and required in input by the SHYFEM model, is provided.

Table 1: Summary description of the forcing, boundary conditions and validation measurements, available for the Pilot Area, market in green, and non-available, marked in orange, which are required in input by the SHYFEM model. The header line show the years the data have been checked for availability.

Boundary conditions	**2017**	**2018**	**2019**	**2020**
Meteorological forcing			up to 31/03	
Rivers flow at mouth				
Open sea boundary and				
Sea currents				
Measurements for validation	**2017**	**2018**	**2019**	**2020**
CDT Gulf (n. of monthly profiles)	16	16	16	16
CTD Lagoon (n. of monthly profiles)	0	0	0	0
CTD Lagoon (n. of seasonally	16	16	16	16

3.2. Transitional and coastal areas in Emilia Romagna (IT)

Sacca di Goro is a roughly triangular, shallow-water lagoon of the Southern Po River Delta covering an area of approximately 26km² with an average depth of 1.5m. Figure 9 shows the geographical area where the lagoon of Sacca di Goro is located. At its Northern portion, the lagoon is surrounded by embankments while it is connected to the Adriatic Sea in its Southern opening. Important freshwater

inputs are represented by the Po di Volano River (approximately 350.106 m3 yr-1), the Canal Bianco and Giralda (both with similar discharge rates of around 20-55 x 106m^3yr^{-1}). Freshwater inlets are also located along the Po di Goro River and are regulated by sluices plus a large channel with unregulated input close to the lighthouse. There are no direct estimates of the freshwater input from Po di Goro, which is usually assumed to be equivalent to that of the Po di Volano. The fresh water or hydraulic residence time oscillates monthly between 2.5 and 122 days with a mean value of 24.5 days, whereas the water exchange time ranges from 2 to 4 days. The tidal amplitude is ca 80 cm. In terms of sediment and geomorphology, the lagoon is majoritarily flat containing alluvial muds with high clay and silt content in its northern and central zones. Sand is more abundant near the southern shoreline, whilst sandy mud occurs in the eastern area. The climate of the region is Mediterranean with some continental influence (wet Mediterranean).

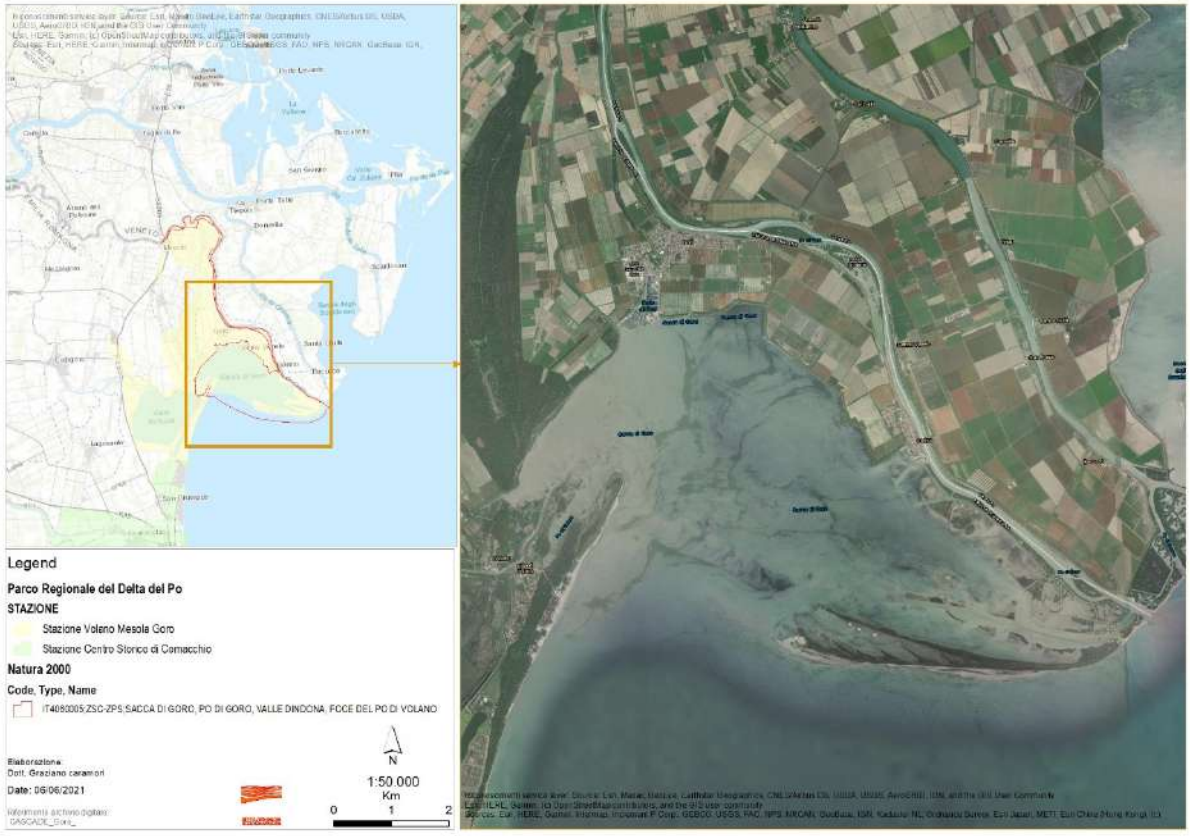

Figure 9. Geographical location of the lagoon of Sacca di Goro

The lagoon of Sacca di Goro is a Natura 2000 site both SPA and SAC (code IT4060005) being also part of the Parco del Delta del Po dell'Emilia-Romagna. Moreover, the eastern area (named Valle di Gorino) is a Ramsar site covering about 1,500ha while the outer bank is a Natural State Reserve.

From an environmental perspective, Sacca di Goro represents a typical coastal lagoon left by the great reclamation carried out in the last 150 years. Ecological peculiarities of this environment allow the

establishment and presence of important plant and animal communities. In the Valle di Gorino area and the border between the Sacca and the Po di Goro, the most widespread marsh formation is the common reed *Phragmites australis*. In the deeper areas of the Sacca even though the submerged vegetation is poor in species, it reaches enormous amounts of biomass (dominated by algae) hosting large planktonic and benthic communities. In more sheltered waters, there have been submerged seagrass meadows (*Ruppia cirrhosa*) that disappeared as in most of the delta. In the area between Goro and Gorino, near the embankment of the former Valle Vallazza, *Gracilariopsis longissima* (= *Gracilaria verrucosa*, red algae) is common.

Geomorphologically, the outer bank delimiting the border with the open sea is in continuous morphological evolution controlled by the sediment influx from the Po river. The outer bank tends to gradually extend towards west, consequently reducing exchanges with the open sea.

As a typical brackish lagoon, the mixture of freshwater and seawater is somehow balanced with Sacca di Goro being categorized as a transitional water body. This feature allows an uncommon biodiversity richness in terms of habitats and species.

In recent years, a joint effort between Arpae, Unibo and CNR-ISMAR made possible the development of an hydrodynamic model of the Goro lagoon called GOLFEM (GOro Lagoon Finite Element Model; Maicu et al., 2021). The system is based on the unstructured grid ocean model SHYFEM (System of HYdrodynamics Finite Element Modules; Umgiesser et al., 2004, Cucco and Umgiesser, 2006) and brings important developments in the study of the Goro lagoon. A high resolution setting was achieved allowing the description of the thin channels connecting the Po of Goro with the lagoon (10 m in the thinner channel) as well as the internal structure of the navigable channels that influence the overall lagoon circulation. The computational grid (figure 3.2.2) has a resolution spanning from 10m (in the narrowest channel) to 2.2 km (at the offshore boundary) with a total of 77496 elements. This approach allows to account for interactions and feedback between large-scale offshore processes and small scale coastal circulation. Moreover, the unstructured grid allows to describe in very detail the complex coastal shape of the lagoon. The wide extension of the domain is needed to cover the whole Po delta, which is the most important freshwater source in the Adriatic sea strongly impacting mass and salt balances (Ludwig et al., 2009). The domain also covers the branches of the Po river in order to adequately represent saltwater intrusion.

In terms of model setting, the water column comprehends 17 vertical levels with a thickness ranging from 1m in the upper 10m, increasing to a maximum thickness of 7m in the last layer. Responding to sea-level variations caused by tides, steric effects and atmospheric forcing, the thickness of the first layer adjusts with time. Finally, the model was calibrated and validated using observations (see Figure 10) of velocity, sea level, temperature and salinity collected in 2018. More details about the model and the results are described in Maicu et al. 2021.

The Goro GOLFEM Circulation model is being integrated with a simple coupling with the biogeochemical fluxes model, BFM. The modelling domain covered by the highly resolved GOLFEM

grid is being divided in a limited number of homogeneous areas (see below) and for each area a 0D version of the BFM will be implemented. Such model will receive inputs about the exchanges among boxes by means of a dedicated routine.

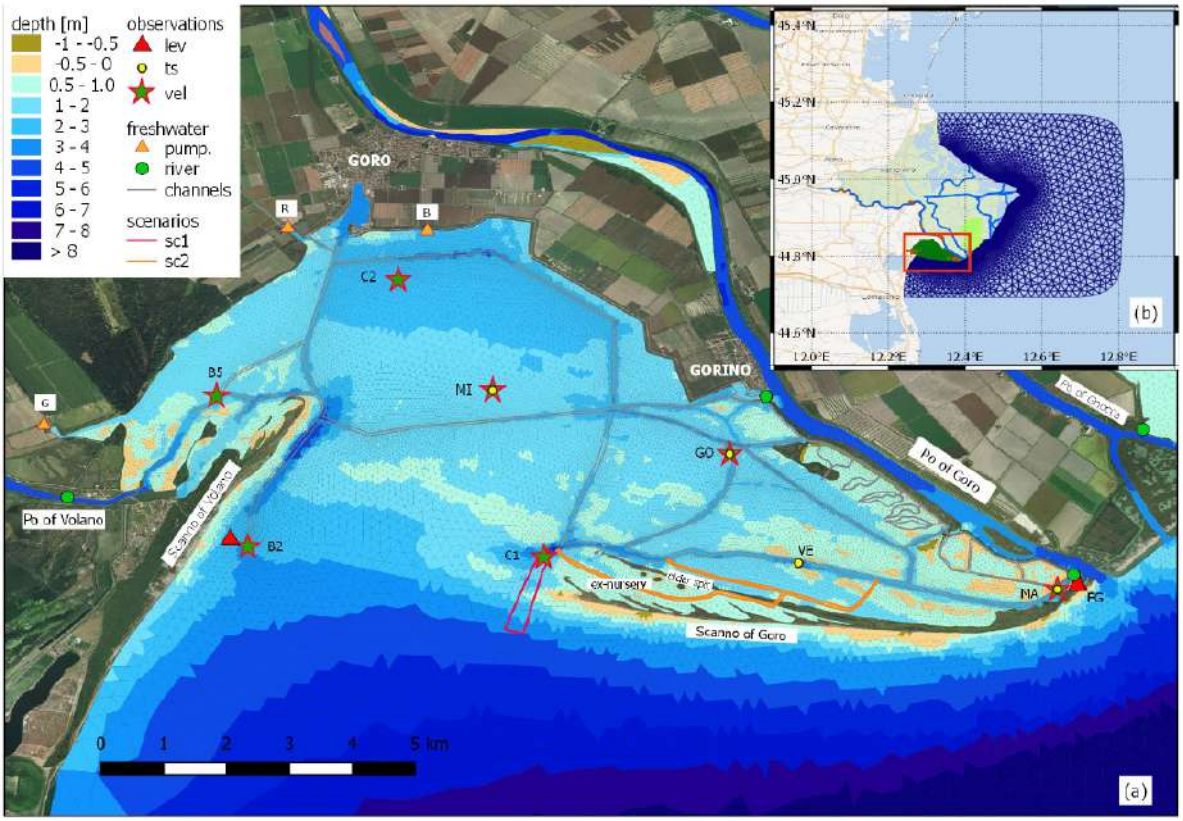

Figure 10: Computational domain of GOLFEM model. a) bathymetry is described by blue contouring, freshwater input and measurement stations are indicated as described in the legend. b) the entire domain is shown.

The biogeochemical runs will be carried out with the BFM model. However, since the total number of nodes in the hydrodynamic model is quite high, it seems unrealistic to simulate the ecological processes on all nodes of the grid. This is especially true due to the fact that many calibration and validation runs will have to be performed for a satisfactory description of the processes.

It has therefore been decided to implement a box model where only some macro-areas will be modelled by the ecological model (see Figure 11). The hydrodynamic model computes the fluxes between the boxes, and the box model will then simulate the bio-geo-chemical reactions inside the single boxes.

The boxes of the box model have been designed in order to assure that every box contains a monitoring station. These data can then be used in the calibration and validation process. Moreover, the boxes

have been chosen to divide the Goro lagoon in already known areas that show different characteristics what concerns the circulation and the ecological processes.

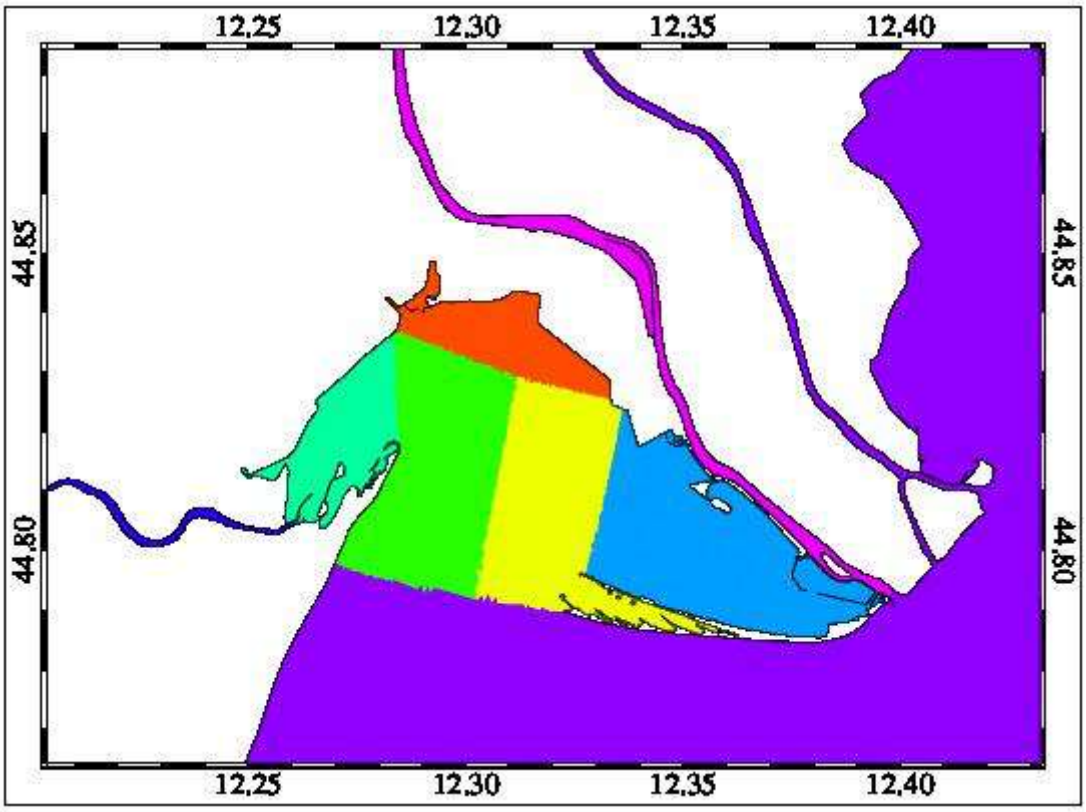

Figure 11: The outline of the boxes to be used in the box model. There are 5 boxes inside the Goro lagoon, 1 box for the southern Po arm, and one box for the rest of the domain, to be used as boundary conditions.

3.3. Torre Guaceto-Canale Reale, Punta della Contessa and Melendugno in Puglia (IT)

The Apulia region is one of the Italian regions with the largest coastal extension (~985 km). The three main categories of the coastal morphology are: (i) rocky coasts (about 31%), such as in the Gargano area; (ii) cliffs called "falesie" (about 22%) which are very steep escarpment due to the strong and continuative erosive action of the sea on the rocky coast with sheer walls; (iii) sandy coasts (about

29%), located in some spots over the entire region, with the largest extension in the southern part of Apulia (e.g. in Gulf of Taranto).

Coastal modelling for the Apulia region in the CASCADE project is mainly focused on the following pilots of Torre Guaceto-Canale Reale, Punta della Contessa and Melendugno. Due to the continuity between the three Pilots and between the hydrodynamic features (e.g. the southward-oriented coastal current Western Adriatic Coastal circulation), we have adopted a seamless modelling approach for the entire Adriatic coastal waters of Apulia. The area covered by the model designed for the Apulia Pilot scale is the Southern Adriatic Sea from 14.6 to 19.9°E and 39.8 to 43.5°N with a horizontal resolution ranging from 2.0km in open sea to 30m at overall Apulian coasts. Figure 3a shows the whole geographical domain, the bathymetry and the overlapped grid, with enlarged views of the grid (Figure 3b and c) including the three Pilots. Also for this case, the model used is SHYFEM and the main modelling setting are similar to the ones descried in section 2.2.

In this stage of model design we have performed a simulation of 2 years (2018-2019). In Figure 13 we report the seasonal-average surface circulation fields and the main open-ocean features (e.g. the Sothern Adriatic Gyre, the Western Adriatic Coastal Circulation). Next steps will foreseen: (i) longer simulation (up to 3-4 years, i.e. 2018-2020/2021); (ii) assess the main features at very local scale (e.g. Pilot scale where the horizontal resolution is 30m) (iii) validation against different observing datasets (satellite SST, ARGO floats, tidegauges); (iii) short-term operational forecasts. These results will be achieved in deliverable D4.2.1 (Models simulations and forecasting systems).

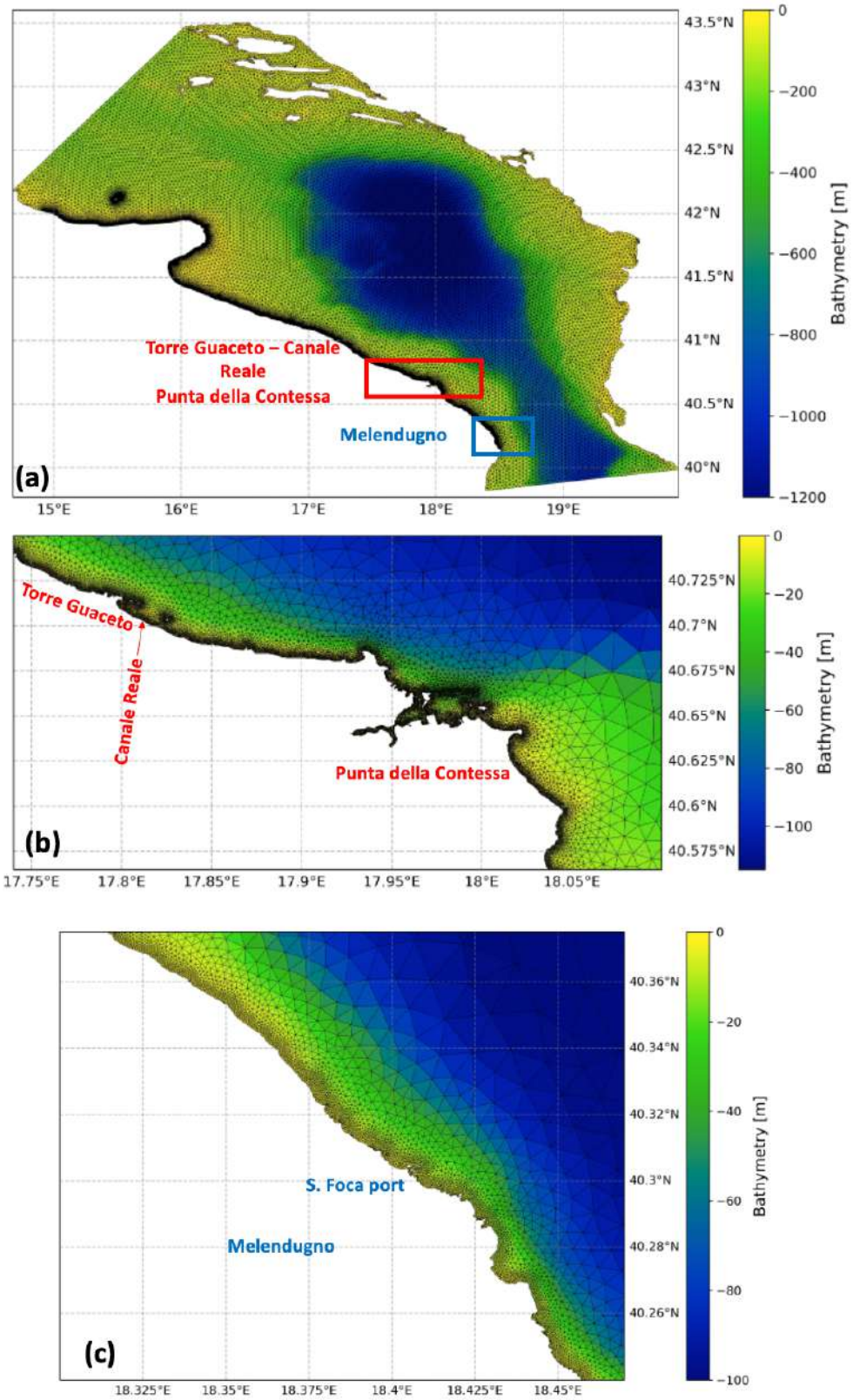

Figure 12: Geographical domain, bathymetry and grid of very high-resolution coastal modelling for Apulia Pilots

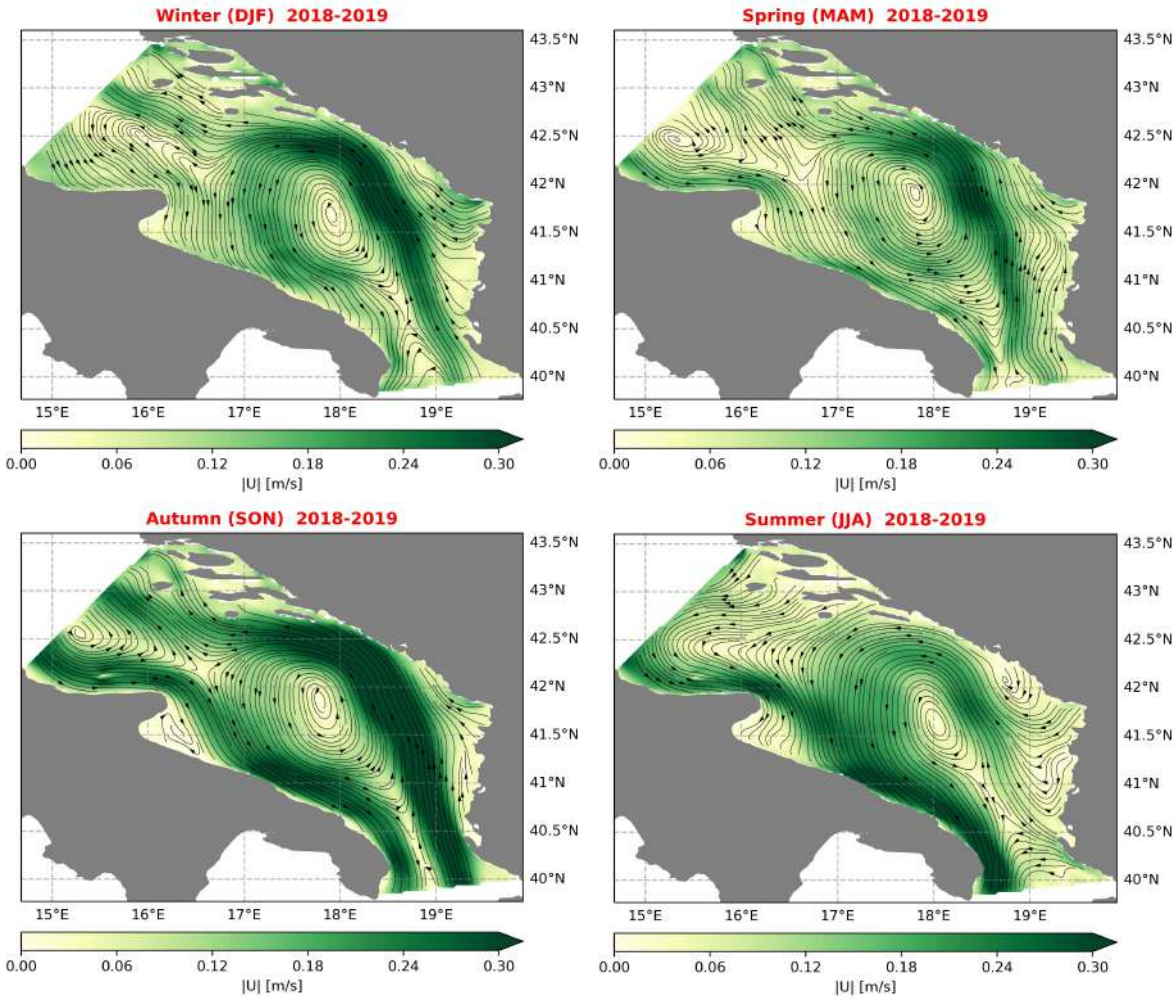

Figure 13: Seasonal-average basin-scale surface circulation in the Souhern Adriatic Sea from very high resolution coastal modelling of Apulia Pilots

3.4. Coastal area in Veneto (IT)

A spatially explicit Ecosystem-based management approach was adopted for the pilot site P5 - Tegnùe di Chioggia. The main goal of the activity consisted in the spatialization of an existing food web model of the northern Adriatic Sea, based on Ecopath with Ecosim, and its downscaling to the 'Tegnùe di Chioggia', for exploring different consequences of different management scenarios.

Ecopath with Ecosim consists of three modules. The first, Ecopath, provides a snapshot of the structure and functioning of the trophic network in a given time period. The trophic network, linked by mass flows (t $km^{-2}y^{-1}$) is represented by various functional trophic groups, which may be single species or species presenting a common trophic or functional behaviour. The basic assumption of this module is the mass balance between the total production of the trophic group (t y^{-1}) and its consumption (t y^{-1}). Ecosim is the temporally dynamic module of EwE; it allows the biomass of individual trophic groups to be monitored over time, simulating prey-predator relationships based on foraging arena theory (Ahrens et al., 2012). Ecosim can calibrate the model based on existing time series and simulate climatic scenarios. Finally, Ecospace represents the dynamic module both temporally and spatially explicit (Walters, 1999; Pauly et al., 2000); the biomasses of individual trophic groups are predicted in space and time according to the habitat foraging capacity model, in which the capacity of each cell in space represents the proportion of the cell on which the group can feed. (Christensen et al., 2014).

For 'Le Tegnùe di Chioggia' (P5 - CASCADE), the Ecopath model structure was largely taken from the version for the northern Adriatic Sea (Libralato et al., 2015): this version included 22 compartments representing primary producers, such as phytoplankton, but also the detritus compartment, macrobenthic groups, zooplankton and fishes (Figure 14). The trophic group Mytilus galloprovincialis (MYT), characterizing the mussel farms present within the study area, and the trophic group Chamelea gallina (CHA), replacing the pre-existing group for the Veneridae family, were added. We also included trophic groups and species characteristics for the biogenic outcrops of the tegnùe:

- Tegnùa primary producers: Lithophyllum stictaeforme, Lithothamnion minervae, Peyssonnelia polymorpha and turf algae;
- Tegnùa filter feeders: Dictyonella incisa, Antho inconstans, Cliona viridis, Tedania anhelans, Epizoanthus spp, Polycitur adriaticus;
- Tegnùa nekton: Pagellus erythrinus, Spicara smaris, Diplodus annularis.

Ecopath parameters, such as biomass over the study area (t km^{-2}), production (t y^{-1}) and consumption rates (t y^{-1}) were left as previously indicated for the northern Adriatic Sea. The biomass for Chamelea gallina trophic group was estimated knowing the % composition of each cited dimensional classes over the total number of individuals in Venice lagoon (CORILA, 2018), and the length – weight relationship for the species (Froglia, unpublished data, cited in Morello et al., 2011). The biomass for Mytilus galloprovincialis was estimated by knowing the mean weight of an individual in a farm over a year (Brigolin et al., 2009) and the final biomass at the harvest season (estimated at 300 t km^{-2}). The model also includes 5 different fleets (different trawling gears, hydraulic dredge, artisanal and recreational fishery).

In our case, no time-series or climate forcing drivers were included in the Ecosim module. Nonetheless, a set of long-term simulations (100 years) were performed to verify that the food web presented a stable behaviour for the relative trophic groups biomasses.

The Ecospace module spatializes the biomass of the trophic groups.

The software is provided with some basic maps, such as the grid of the study area, bathymetry map (EMODnet Bathymetry Consortium) and primary productivity (Generated using E.U. Copernicus Marine Service Information). The maps have been inserted with a resolution of 1km (Figure 15).

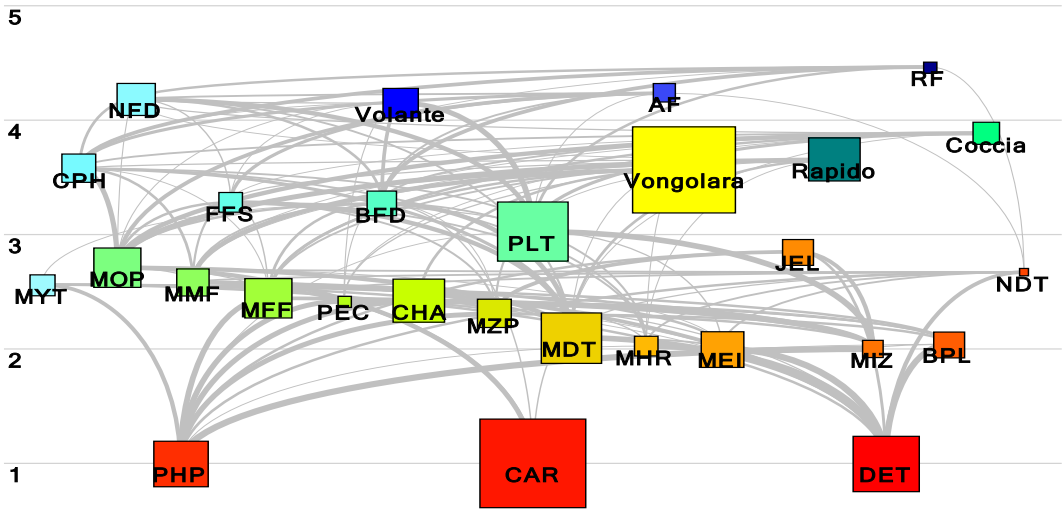

Figura 14:The flow diagram of the food web modelled in EwE provided by Ecopath tool; Phytoplankton (PHP); Mytilus galloprovincialis (MYT); Macrobenthic Predators (MOP); Macrobenthic Mixed Feeders (MMF); Macrobenthic Filter Feeders (MFF); Pectinidae (PEC); Chamelea gallina (CHA); Macrozooplancton (MZP); Macrobenthic detritivorous (MDT); Macrobenthic herbivores (MHR); Meiobenthos (MEI); Microzooplankton (MIZ); Bacterioplankton (BPL); Jellyfish (JEL); Nekton detritivorous (NDT); Planktivorous feeders (PLT); Benthic feeders (BFD); Flat fishes (FFS); Cephalopods (CPH); Nekton feeders (NKT); for the fleets Volante, Vongolara, Rapido; Coccia; Ricreative fishing (RF); Artisanal fishing (AF); Carcass (CAR); Detritus (DET).

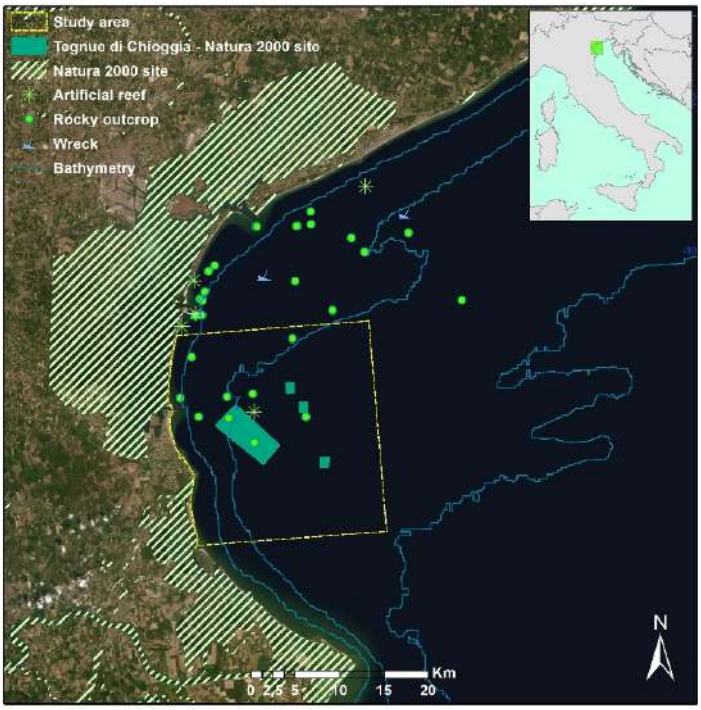

Figura 15: The spatial context of the study area. The study site modelled in Ecospace is the portion of sea within the dashed yellow line. The green polygons represent the SCI “Tegnùe di Chioggia”, while the green dots are biogenic rocky outcrops.

Each trophic group can be spatialized by being assigned to specific habitats within the study area, or by its tolerance responses to different environmental drivers; the combination of the environmental responses constitutes the "capacity" of each grid cell to forage the trophic group (value from 0 to 1); the capacity then determines the distribution of trophic group biomass in space.

Both options were used in our case.

Four different habitats were created in the study area based on sediment type and the presence or absence of mussel farms:

- Mussel farms habitat: habitats characterized by the presence of mussel farms in the water column (% cell coverage; Mariculture - Adriatic Sea from Tools4MSP; Menegon et al., 2018).
- Sandy habitats: habitats with a predominantly sandy bottom (% cell coverage, EMODnet Seabed substrates 7 folk)
- Habitat muddy: habitat with a predominantly muddy seabed (% cell coverage, EMODnet Seabed substrates 7 folk)

- Habitat rocky: habitat characterized by the presence of rocky outcrops.(% cell coverage; Ponti, 2020, (a)(b)(c); Fortibuoni et al., 2020, (a)(b); Gordini et al., 2020; Andreoli et al., 2010).

The groups susceptible to the presence of such habitats were given a coefficient from 0 to 1 for each of them; this coefficient describes the % of a cell characterized by a given habitat type on which the group can feed.

In the case of Chamelea gallina and the Pectinidae family trophic group, the spatialization of the biomass was driven by the relationship between the relative abundance of the species according to bathymetry (CORILA, 2018; Fishbase.org).

The fishing effort of the fleets included in the Ecopath module was also spatialized. This was performed on the basis of AIS (Automatic Identification System) tracking data of the vessels that set sail from Chioggia in the northern Adriatic Sea (Russo, E., 2020). Fishing effort is quantified as the % of a 1kmx1km grid cell scanned during the active fishing phase by the vessel, averaged over 2015 and 2016 years. As an example, a fishing effort for the Volante fleet of 500% means, that, on average, the fleet completely scanned the cell 5 times during the 2015-2016 fishing seasons. The maps were then normalized (fishing effort value between 0 and 1) and entered as "sailing cost" in Ecospace (sailing cost = 1 – effort).

Within the study area, two fishing closure zones, where fishing activities are prohibited at any time of the year, were mapped as presence-absence data points, respectively, the Tegnùe di Chioggia SCI and the area closed to trawling within 3 miles from the coast.

The main outputs of the Ecospace module are biomass (for trophic groups) or catch (for fleets) variation (t km^{-2}) in space and time (Figure 16 and 17), and functional ecological indicators.

The tool is therefore used to test its potentiality in evaluating the effectiveness of different management scenarios within CASCADE:

- Expansion of the Tegnùe di Chioggia ZTB;
- Partial openings for artisanal and ricreative fishing within the Tegnue di Chioggia;
- Expansion/reallocation of existing mussel farms.

Here we report some relevant information for the application. The bathymetric metadata and Digital Terrain Model data products have been derived from the EMODnet Bathymetry portal - http://www.emodnet-bathymetry.eu. Information about seabed habitats here has been derived from data that is made available under the European Marine Observation Data Network (EMODnet) Seabed Habitats initiative (http://www.emodnet-seabedhabitats.eu/), financed by the European Union under Regulation (EU) No 508/2014 of the European Parliament and of the Council of 15 May 2014 on the European Maritime and Fisheries Fund. Primary productivity maps have been derived from Mediterranean Sea Monthly and Daily Reprocessed Surface Chlorophyll Concentration from Multi Satellite observations + SeaWiFS daily climatology, available at

https://resources.marine.copernicus.eu/product-detail/OCEANCOLOUR_MED_CHL_L4_REP_OBSERVATIONS_009_078/INFORMATION.

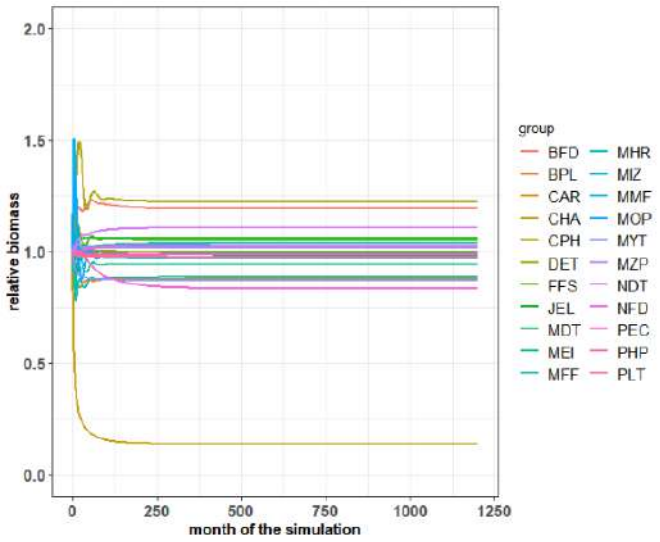

Figura 16. Timeplot of biomass variation (t km^{-2} over the study area) for each trophic group obtained after the Ecospace simulation (in log scale).

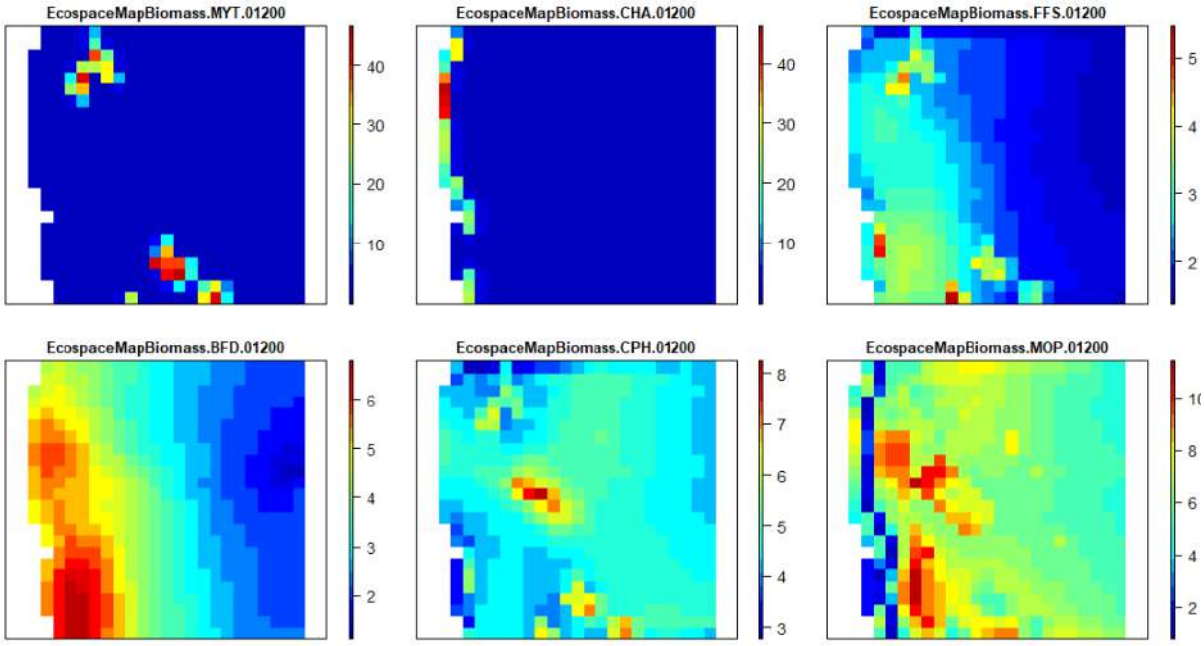

Figure 17. Spatially explicit biomass maps (t km-2) for some of the trophic groups (Mytilus galloprovincialis, Chamelea gallina, Flat Fishes, Benthos Feeders, Cephalopods and Macrobenthic Predators) after running the simulation in Ecospace in an eutrophication scenario.

3.5. Miljašić Jaruga river mouth, Nin bay (HR)

The Miljašić Jaruga watercourse flows into the sea at Nin Bay. The final section passes through the urban area of the City of Nin. Its riverbed is partially covered with sediment, untidy, overgrown with grass and low vegetation. The existing stone reinforcement is damaged and, on some sections, has completely collapsed. Collapsed structures and deposited sediment reduce the flow profile of the watercourse and sometimes cause backwater. The mouth of the Miljašić Jaruga itself, which is going to be restored through this pilot project, consists of two groynes, east and west, both in very poor condition. Currently, the eastern groyne is constructed like a vertical coastal wall that allows for an occasional (summer) berth (approximately 30 m long). The other side is formed as a sloping shore made of hand-stacked stones (36 m long) and is in poor condition. The groyne's crown is also made of hand-stacked stone, with some parts damaged and stones missing. The armor layer on the outside of the east groyne is in a rather poor condition. The western groyne was constructed as a rock embankment reinforced with an armor layer, but over time it is destroyed. Figure 18 shows the area of interest with the location of Miljašić Jaruga mouth and preliminary design of the groins.

The project area covers about 2.5 ha of sea and coastal area. The Miljašić Jaruga mouth is in an area of rich cultural, historical, and archaeological heritage and represents a valuable area, which requires complete landscaping. In addition to the primary purpose of protecting against flooding, it will have an aesthetic purpose like the rest of the area. Additionally, the mouth is a part of the Natura 2000

ecological network area, which is important for habitats and species, especially for birds. A Mediterranean climate with hot summers prevails in the area with average day temperatures in the warm moths exceeding 22 °C. The area of the Miljašić Jaruga basin is 131 km^2, and the highest recorded freshwater discharge equals 47 m^3/s.

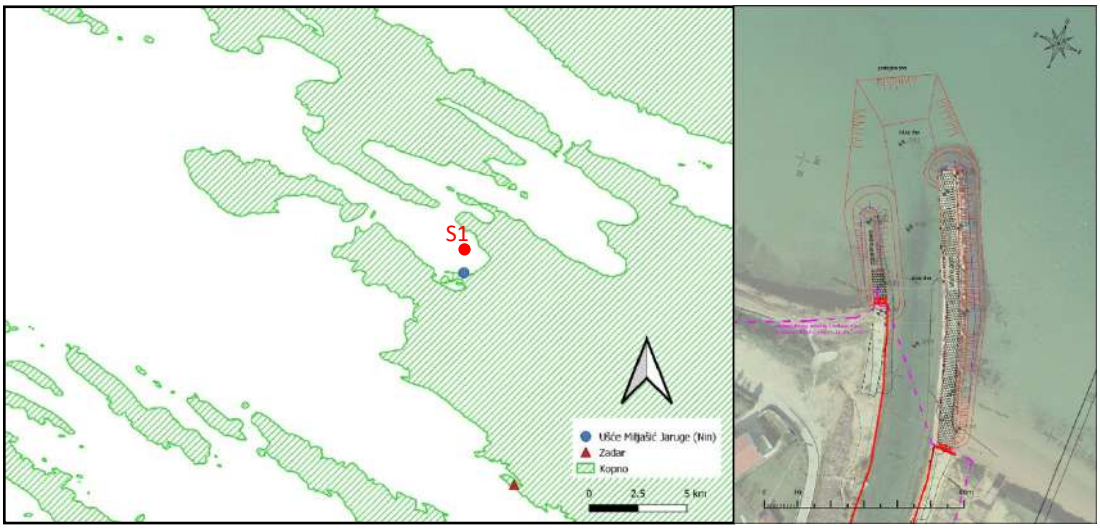

Figure 18. Map showing the location of Miljašić Jaruga mouth and preliminary design of the groynes

The wind climate for the city of Nin was determined on the basis of a long time series of measurements of wind velocity and direction at the main meteorological station Zadar. The series used covers the time period from July 1995 to February 2021, and contains average hourly values of wind velocity expressed in meters per second and wind direction for 16 main directions. The most common wind at GMP Zadar is the levant (the wind from the east). In addition to the levant, the city of Nin will be affected by the bora, mistral, and tramontana. Due to the orientation of the coast along the city of Nin to the north and at the mouth of Miljašić Jaruga, further analysis will include action from these three wind directions for wave forecasting. Figure 19 shows the wind rose with wind velocity by directions based on 26 years of data from the main meteorological station in Zadar. Table 2 shows the associated sectors, wind names and directions expressed in degrees and direction marks.

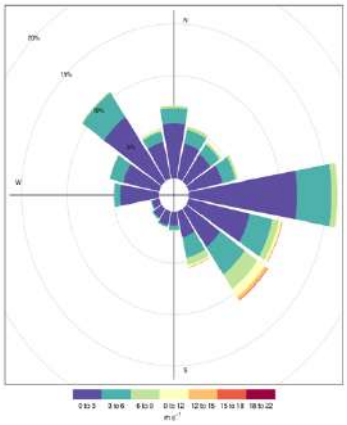

Figure 19. Wind rose - wind velocity by directions based on 26 years of data from the main meteorological station in Zadar.

Table 2: Associated sectors, wind names and directions expressed in degrees and direction marks.

Sector	I	II	III
Wind	Mistral	Tramontana	Levante and Bora
Direction (°)	[270°, 330°]	<330°, 30°]	<30°, 90°]
Direction	W, WNW i NW	NNW, N i NNE	NE, ENE i E

Sea currents represent the directed movement of water mass within the sea water column. In general, currents in the sea are formed under the influence of various causal forces. Some could be made up of gradient currents caused by horizontal differences in sea density, currents resulting from tidal forces, and shear currents generated by wind on the sea surface. In addition, the currents in a given basin are significantly affected by its dimensions as well as the topographic features of the coast and the seabed. The general movement of water masses in the Adriatic Sea takes place counterclockwise (cyclonic). Knowledge of the properties of currents and surface sea waves in an area is important for a large number of activities, and as currents and waves are the basic factors of sediment transport, it is important to know them in order to define interventions to prevent unwanted sediment movement. The measurements were performed with a ADCP probe, continuously over a longer period of time (30 days), thus obtaining a time distribution of sea current velocities and surface waves. The set of time series enables a more comprehensive overview and understanding of sea hydrodynamics. Sea current measurements were performed with an ultrasonic current meter (ADCP-Monitor 600 kHz, RDInstruments, USA). Measurements with the ADCP probe in the Bay of Nin were performed at point

S1 (f = 44.27 °, l = 15.18°; fig.1), (average depth 9m), in the period from 23.09.2009-15.10.2009. The obtained time series of vectors of sea current velocity, were statistically processed and the basic statistical parameters shown in the table below were obtained (Tab 2). The column 'depth_avg' shows the statistical parameters for the time series of velocity vectors averaged by depth.

The maximum measured speed is 22.3 cm / s in the surface layer (d = 2m), and the lowest in the bottom layer is 16.8 cm7s (d = 7m). Mean speeds are uniform throughout the water column ~ 4cm / s. The resulting vector has the highest value in the bottom layer d = 7m, 1.8 cm / s, while in the middle and surface layer it is smaller 1.6 cm / s. The resulting vector obtained as the resultant in depth and time equals to 1.6 cm/s and a direction of 159°, which means that the flow is predominantly in the SSE direction. All the statistical parameters of measured sea currents are reported in Table 3.

It is concluded that sea currents are too low to significantly contribute to longshore and crosshore sediment transport. The main driver of sediment transport is concluded to be wave action and shore breaking, so more attention will be given to it in the following section.

Table 3: Statistical parameters of measured sea currents in the period from 23.09.2009. to 15.10.2009, for depths d = 2, 5 and 7m and for a depth averaged vector time series ('depth_avg'), for measuring point f = 44.27 °, l = 15.18 °

depth	d=7m'	d=5m'	'd=2m'	'depth_avg'
Max.velocity (cm/s)	16.8	20.0	22.3	19.2
Average velocity (cm/s)	4.0	3.9	4.1	2.9
St. Dev. (cm/s)	2.5	2.4	2.6	2.1
Resulting vector (cm/s)	1.8	1.6	1.6	1.6
Resulting vector direction (°)	140	159	167	159

To determine the wave height, wind data are needed - a long-term record of the wind velocity and direction as well as the fetch lengths over which the wind generates waves. The wind data used in this study were measured at the main meteorological station in Zadar for the period from April 1995 to February 2021. Hourly values were used for wind velocity expressed in m/s, and for wind direction from 16 different directions. The main meteorological station in Zadar is the nearest station with a long-term record. The fetch length is determined by averaging the distance of the point of interest from the shore in the direction of the sector from which the wind blows, and is determined for several different directions of wind flow. For the purpose of calculating the fetch length, one point of interest was used, and it is located in front of the mouth of the watercourse Miljašić Jaruga.

The maritime structure's design was developed considering the wind and wave climate. The numerical wave model for the Miljašić Jaruga mouth was developed in the Aquaveo SMS (Surface-water Modeling System, SMS) software package. The model is based on the refraction-diffraction equation applied to long and short waves and thus finds wide application for models related to coastal engineering. Since the equations are elliptical, the model solves a steady-state problem forced by boundary conditions. This is a good basis for performing wave simulations in urban and natural basins with an arbitrary depth variation, without restriction on the wave approach angle. This represents a complete two-dimensional wave problem for the inhomogeneous Helmholtz equation. Wave deformations that CGWAVE can simulate are refraction, diffraction, reflection (from coastal structures and natural boundaries (breakwater, coast, etc.)), friction, and wave breaking. The model uses a triangular mesh of finite elements of different sizes over the entire area corresponding to the local wavelength. The model allows setting the desired value of the reflection coefficient along the coast

and other boundaries. Although the basic equations are intended for monochromatic waves, irregular (i.e., spectral) waves are simulated in CGWAVE through a linear superposition of monochromatic simulations. To calculate the waves, the model uses a semicircle as an open boundary to define the domain of the model. The tidal oscillation range is about 30 cm. Wind directions that dominate are NE and SE during the winter and NW during the summer. The wave climate for several directions and two distinct return periods is presented in Table 4.

The different sensitivity tests performed with current state and with constructed state configuration are reported in Figures 20-21. Furthermore, Figure 22 describes the surface elevation. After the numerical model analysis, we acne determine the design wave parameters (Table 5).

Table 4. Numerical model tests for the current mouth state and new constructed mouth state

Test	Return period (year)	H_s (m)	L_p (m)	T_p (s)	T_s (s)	H_{max} (m)	L_s (m)	Direction [°]
1	5	0.85	21.25	3.69	3.43	1.53	21.26	320
2	100	1.45	36.25	4.82	4.48	2.61	36.27	320
3	5	0.85	21.25	3.69	3.43	1.53	21.26	305
4	100	1.45	36.25	4.82	4.48	2.61	36.27	305
5	5	0.7	17.5	3.35	3.12	1.26	17.52	0
6	100	0.85	21.25	3.69	3.43	1.53	21.26	0
7	5	0.7	17.5	3.35	3.12	1.26	17.52	335
8	100	0.85	21.25	3.69	3.43	1.53	21.26	335

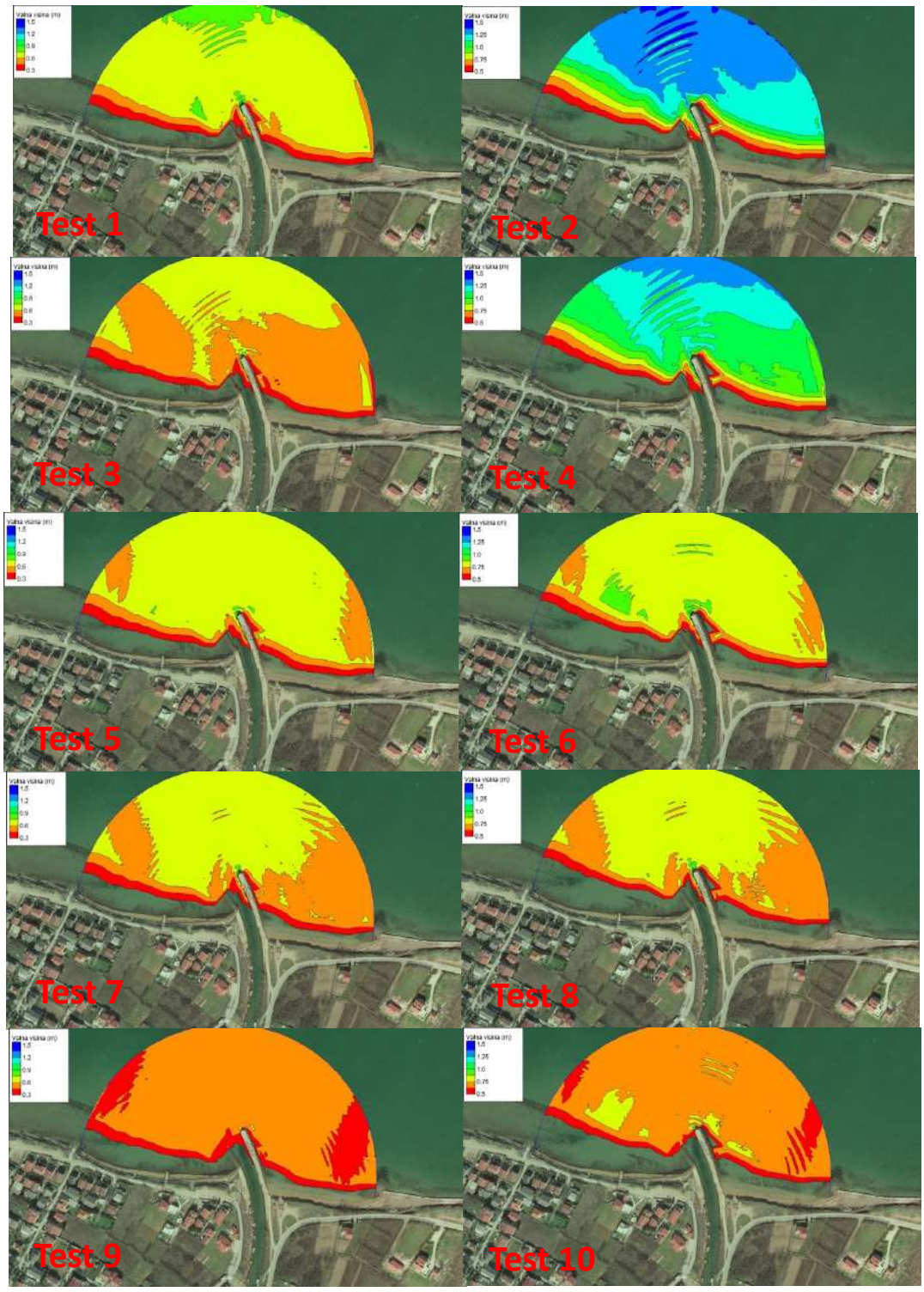

Figure 20. Different tests with current state

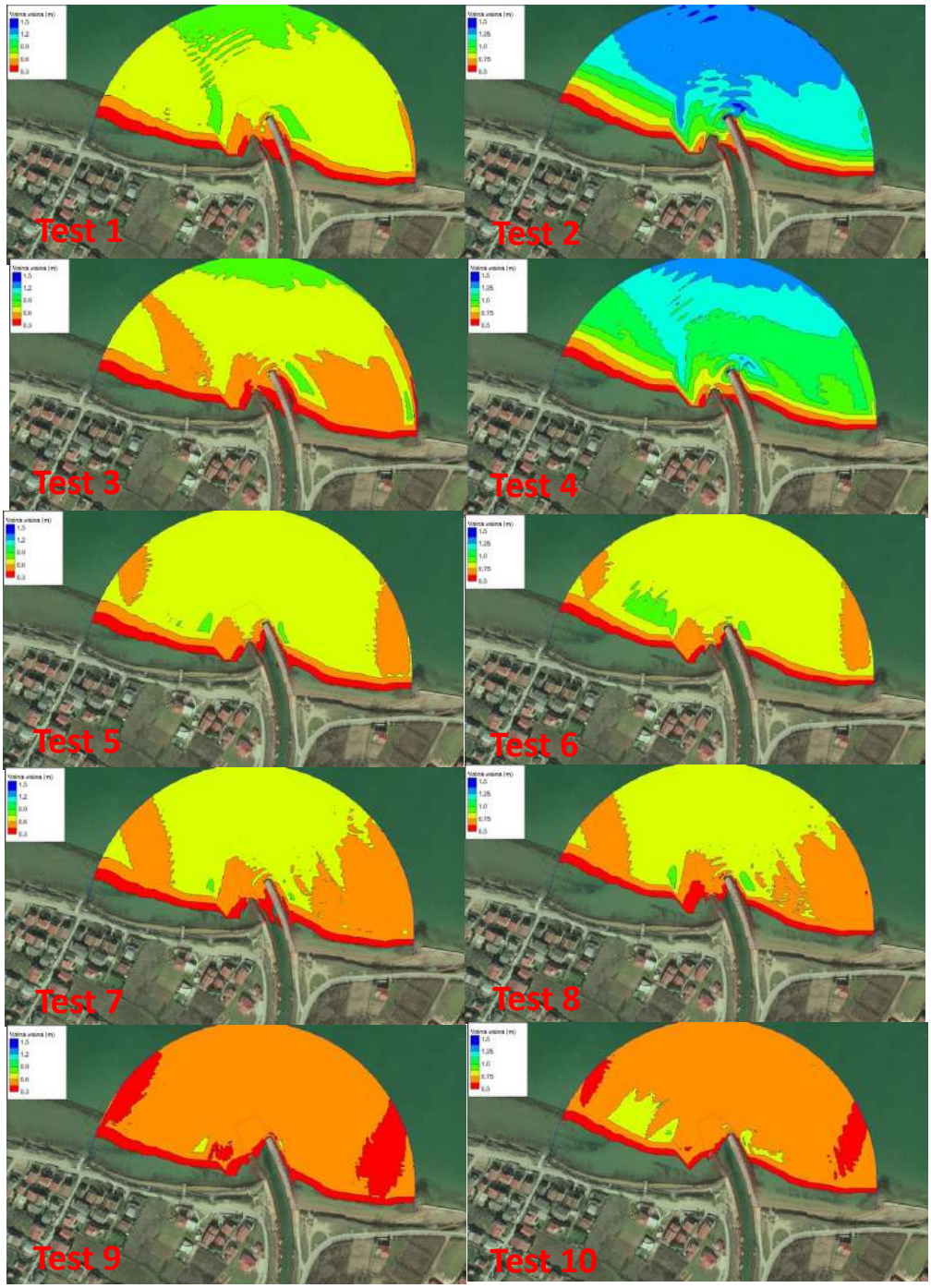

Figure 21. Different tests with constructed state

Figure 22. Surface elevation: Test 1 and Test 2

Table 5. Design wave parameters determined after numerical model analysis

	Groyne head (armor layer)	Groyne (armor layer)	Vertical wall	Rubble beneath the vertical wall (for dissipation)
Eastern groyne	H_s^{100g}=1,5m (breaking wave)	H_s^{100g}=0,85m (breaking wave)	Northern half: H_s^{100g}=1,3m (non-breaking wave) Southern half: H_s^{100g}=0,85m (non-breaking wave)	Northern half: H_s^{100g}=1,3m (non-breaking wave) Southern half: H_s^{100g}=0,75m (non-breaking wave)
Western groyne	H_s^{100g}=1,25m (breaking wave)	H_s^{100g}=0,85m (breaking wave)	H_s^{100g}=0,6m (non-breaking wave)	-

3.6. Coastal area in Molise (IT)

In Biferno river mouth-Campomarino Coast (Pilot Area 7), UNIMOL developed a static model of coastal salt marshes, profiling and describing zonation and conservation status of the most important habitats occurring in the area.

Description of the salt marshes mosaic zonation

Coastal salt marshes are mosaics of low-growing plant communities' dominated by herbaceous plants, which are periodically flooded in relation to the lunar cycle and to local topography. The influence of tides on coastal vegetation depends on the relative duration of submergence and exposure (Adam 1990; Packham & Willis 1997). The distribution pattern of the different plant communities conforming salt marsh mosaics includes zones with the youngest formations placed in lowest sectors, while the oldest occur at the top. In salt marshes, also the depth of brackish water table determines vegetation zonation. Each of the main landform types contains a variety of specialized habitats according to micro-

relief and flooding periodicity (Deil 2000). The number of species on each plant community is often low, with monospecific stands being quite common. High salinity and low soil oxygen are harsh environmental filters that allow the presence of few specialized species. Indeed, few plant species are able to tolerate a high salt concentration in the soil solution or low soil redox potentials (Cutini et al., 2010a).

Coastal salt marshes of the Biferno Mouth (P7) are characterized by a sequence of natural ecosystems that are widespread across the Italian coast and representative of the Mediterranean vegetation zonation. A specific mosaic of halophilic and semi-halophilic vegetation encompasses the fore-dune wetlands, coastal lagoons and geo-morphological variability. The shallow water lagoon often dries up in summer, exposing loamy and salty soils. In the Biferno mouth, we registered the presence of six plant communities articulated in a tinny mosaic responding to morphological variability and heterogeneous pattern of soil salinity.

The most alophile communities occur in the lagoon and along its banks, given by aquatic vegetation with Ruppia spiralis (EU habitat 1150*) and with Salicornia fruticosa (EU habitat 1420). Mediterranean salt steppes with a Limonium narborense and Aster tripolium (EU habitat 1510*) occur in close contact with Salicornia sp. formation in slightly higher areas. In the fore-dunes salty depressions, we registered a mosaic of Mediterranean salt meadows with Juncus maritimi (EU habitat 1410) and the Mediterranean temporary ponds (EU habitat 3170*), which are detectable only in winter or late spring. Such formations are characterized by Mediterranean therophytes and geophytes taxa. Close to coastal dune vegetation on sandy-clay soils, we observed Mediterranean tall humid herb grasslands with Erianthus ravennae (EU habitat 6420).

Conservation status

The conservation status of the coastal salt marshes of the Biferno Mouth is good, as evidenced by the presence on six habitats of conservation concern in Europe, each one with a good pool of diagnostic species according to the Habitat directive (Biondi et al 2009).

Vegetation structure is similar to other not-disturbed areas in Italy (Cutini et al 2010b) and Europe. Still, the occurrence of some alien plants as Aster squamatum, Erigeron canadensis and E. sumatrensis, underlines the presence of anthropic pressures that require to be monitored over time. Coastal salt marshes are also impinged by tourism from the seashore and agriculture from the inner coastal plains with most of the cultivated filed gained to natural marshes by reclamation infrastructures built up over 50 years ago (Stanisci et al., 2008). Furthermore, like all the coastal ecosystems, salt marshes are threatened by climate change as the rising of the sea level could raise the brackish water tables, dramatically altering the coastal salt marshes mosaic (Iannantuono et al., 2004; Aucelli et al., 2008).

Management scenarios

To assure a good conservation status of salt marshes in the Biferno river mouth by e.g. reducing the propagule pressure of alien species given by human trampling and the presence of paths and walkways, some soft conservation actions could be implemented. For instance, the creation of green infrastructures given by hedges and planted tamarisks bordering the lagoon could help to filter alien species dispersion (propagule pressure) from artificial areas and access routes.

Such soft conservation action should also contribute to improve the naturalistic value of the area, which is also extremely important for bird (i.e. a huge number of migratory and sedentary birds), reptile (i.e. Hemys orbicularis) and bat species (https://lifemaestrale.eu/), most of which are of conservation concern in Europe and worldwide. Green infrastructures could also help to delimit the salt marshes from the nearby cultivated fields, as to curtail the effects of pest control products used in agriculture (insecticides), which can pollute waters and soils with deleterious effect on marshes biodiversity.

The good conservation conditions of the Biferno mouth salt marshes are due to a dedicated conservation action implemented by the LIFE MAESTRALE project (https://lifemaestrale.eu/). The excavation of an underground pond allowed to re-establish the original wetland and the natural water flow from a drainage channel. This has favored the reinstatement of the original hydrological conditions of the ponds and the improvement of environmental conditions. Fascines in plant material were installed parallel to the coastline in order to promote the accumulation of sand carried by the wind and consequently, to mitigate coastal erosion.

Salt marshes in the Biferno mouth are conformed by a mosaic of habitats of conservation concern (habitat Directive 92/43/CEE; http://vnr.unipg.it/habitat/index.jsp) reported schematically in Figure 23 and briefly described below.

EU Habitat 3170*: Mediterranean temporary ponds.

Very shallow temporary ponds (a few centimeters deep) that exist only in winter or late spring, with a flora mainly composed of Mediterranean therophytic and geophytic species (Figure 24).

These formations occur in coastal areas and internal salt areas in Italy and are part of the Alleance *Isoëtion*, *Preslion cervinae*, *Agrostion salmanticae*, *Nanocyperion*, *Verbenion supinae* (= *Heleochloion*) and *Lythrion tribracteati*, *Cicendion* and/or *Cicendio-Solenopsion*.

The main species are of this habitat are: *Juncus bufonius, J. capitatus, J. pygmaeus*

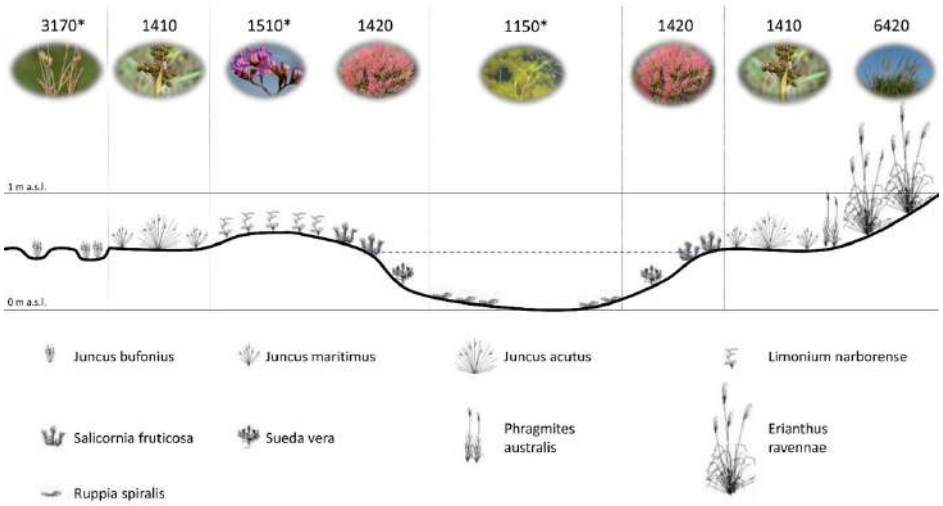

Figure 23. Schematic profile describing the typical Mediterranean coastal salt-marsh zonation present in Biferno river mouth-Campomarino Coast (P7) area and the EU habitat types codes (EU, 1992). The detailed description of the habitats is reported below in the main text.

Figure 24. Picture of the Mediterranean temporary ponds (EU Habitat 3170* of priority conservation concern in Europe) in the Biferno mouth (Pilot area 7). Photo: Francesco Pio Tozzi.

EU Habitat 1410: Mediterranean salt meadows (*Juncetalia maritimi*):

Plant formations of halophiles and sub-hallopilles plants ascribable to the *Juncetalia maritimi* order (Figure 25). It includes a group of salt meadows dominated by rushes and other hygrophilous species. These mosaic occurs on wet fore-dunes on sandy substrates yearly flooded by brackish water for medium-long periods. Mediterranean salt meadows are present on low coasts in the Mediterranean and is present on most of the Regions facing the sea.

Mediterranean salt meadows habitat is distributed along the low coasts of the Mediterranean and in Italy is present in various stations: in almost all the regions facing the sea.

The main species are: *Juncus maritimus, J acutus, Limbarda crithmoides, Artemisia coerulescens, Plantago crassifolia e Schoenus nigricans.*

Figure 25: Picture of the Mediterranean salt meadows (*Juncetalia maritimi* EU Habitat 1410) in the Biferno mouth (Pilot area 7). Photo: Marco Varricchione.

EU Habitat 1420: Mediterranean and thermo-Atlantic halophilous scrubs (*Sarcocornetiea fruticosi*)

Perennial vegetation of marine saline muds mainly composed of succulent camephytes and nanophanerophytes essentially with a Mediterranean-Atlantic distribution (*Sarcocornia* sp and *Arthrocnemum* sp) and belonging to the *Sarcocornetea* fruticosi class (Figure 26).

They form paucispecific communities, on inundated areas, with hyper-saline and meso-saline clayey soils, characterized by the succession of inundated and long dry periods. They constitute an important nesting site for birds.

The main plant species on perennial vegetation of marine saline muds are: *Salicornia fruticosa, Sueda vera, Halimione portulacoides, Limbarda crithmoides.*

Figure 26. Picture of the Mediterranean and thermo-Atlantic halophilous scrubs (*Sarcocornetiea fruticosi* - Habitat 1420) in the Biferno mouth (Pilot area 7). Photo: Francesco Pio Tozzi.

EU Habitat 1510*: Mediterranean salt steppes (*Limonietalia*)

Mediterranean salt steppes in Italy are salt meadows characterized by perennial herbaceous species mainly referable to *Limonium* sp taxa, sometimes coexisting with *Lygeum spartum*. This habitat occurs on coastal areas, on the fringes of salt depressions, and coastal fore-dunes.

Salt steppes growth on salty clay soils that could contain a small part of loam or sand. Salt steppes soils are temporarily wet, occasionally submerged. Their humidity and salt content are regulated by the seasonal variation of the brackish water table. On Mediterranean areas, these steppes, are affected by a pronounced summer dry stress promoting the formation of salt efflorescences and crusts.

The main plant species on Mediterranean salt steppes are: *Limonium narborense* and *Aster tripolium*

EU Habitat 1150*: Coastal lagoons

Coastal aquatic environments with swallow lentic, salty or brackish water (Figure 27). Coastal lagoons are characterized by a pronounced seasonality due to the interplay of rainfalls, evaporation, the intake of fresh seawater from storms, temporary flooding of the sea in winter or tidal exchanges.

Coastal lagoons are stretches of shallow coastal salt water, of varying salinity and water volume, wholly or partially separated from the sea by sand banks or shingle. Lagoons salinity ranges from brackish water to hypersaline which depends on rainfalls, evaporation rates and the variable imput of seawater and tidal dynamics.

The main plant on coastal lagoons is *Ruppia spiralis*.

EU Habitat 6420: Mediterranean tall humid herb grasslands of the *Molinio-Holoschoenion*

Mediterranean reeds and hygrophilous herbaceous formations of tall grasses referable to the *Molinio-Holoschoenion* growing on coastal systems on sandy-clayey soils and rich on stress tolerant species.

The main species of Mediterranean tall humid herb grasslands is the l'*Erianthus ravennae*

Figure 27. Picture of the Mediterranean salt steppes (EU Habitat 1510* of priority conservation interest) in the Biferno mouth (Pilot area 7). Photo: Marco Varricchione.

3.7. Torre del Cerrano, Pineto, Abruzzo (IT)

In Torre del Cerrano (P10), UNIMOL developed a static model of coastal dunes, profiling and describing zonation and conservation status of the most important habitats occurring in the area.

Coastal dunes are sandy habitats located between the sea and the land, thus representing a transition belt between two realms. Accordingly, it is highly dynamic and hosts valuable biodiversity. The morphological instability of dune structure, the soil incoherence and the strong environmental stress as well as the peculiarity of plant species building and stabilizing the sand dunes, make these transition zones unique habitats worldwide (Acosta & Ercole, 2015). Coastal dunes continuously change in response to sea level rise, natural erosion, climate change, fire, cattle and land transformations. However, the typical resilience of dune vegetation often offers a rapid short-term recovery as soon as

the disturbance is interrupted or mitigated through simple management options, as the use of fence or boardwalks.

In well preserved areas, coastal zonation in Torre Cerrano MPA (Pilot 10) is characterized by a sequence of natural ecosystems widespread across the Italian coast and representative of the Mediterranean vegetation. Such ecosystems, all of conservation concern in Europe (Feola et al. 2011; Angelini et al. 2016) are: Annual vegetation of drift lines (EU code:1210), Embryonic shifting dunes (EU code: 2110), Shifting dunes along the shoreline with *Ammophila arenaria*, also called white dunes (EU code: 2120), *Malcolmietalia* dune grasslands (EU code 2230) and Wooded dunes with Pinus pinea and/or Pinus pinaster (EU code: 2270) (Figure 28). These habitats are highly related to variations in substrate coherence, wind action and environmental stress along the sea-inland gradient (Acosta et al. 2003; Drius et al. 2013). Two of them (i.e. fixed dunes and wooded dunes) are a priority of conservation interest at European level and three of them (embryo dunes, mobile dunes and fixed dunes) are currently in poor conservation status in Italy and in Europe (EEC 2013), requiring specific conservation actions.

Here follows the coastal dune zonation with habitats occurring in P10.

EU Habitat 1210: Annual vegetation of drift lines

The habitat 1210 (Figure 29) consists on plant communities conformed by annual species and few perennials, occurring on small accumulations of drift material and gravel rich in nitrogenous organic matter (*Cakiletea maritimae*) (Manuale Italiano di interpretazione degli habitat della Direttiva 92/43 CEE - http://vnr.unipg.it/habitat/index.jsp)

EU Habitat 2110: Embryonic shifting dunes

Formations of the coast representing the first stages of dune construction, constituted by ripples or raised sand surfaces of the upper beach or by a seaward fringe of small embryonic dunes at the foot of the tall dunes (Figure 30). This habitat consists of pioneer communities, dominated by *Elymus farctus*, which represent the first stages of plant colonization and contain some therophytes belonging to annual vegetation of the drift line (Manuale Italiano di interpretazione degli habitat della Direttiva 92/43 CEE - http://vnr.unipg.it/habitat/index.jsp).

EU Habitat 2120: Shifting dunes along the shoreline with Ammophila arenaria (white dunes).

Taller mobile dunes forming the seaward cordons of dune systems, colonized by a perennial herb community dominated by the rhizomatous tussock grass *Ammophila arenaria* ssp. *Australis* (Figure 30). This habitat is generally in sequential contact with the embryonic shifting dunes on the seaward side and with the fixed dunes on the landward side (Manuale Italiano di interpretazione degli habitat della Direttiva 92/43 CEE - http://vnr.unipg.it/habitat/index.jsp).

EU Habitat 2230: Malcolmietalia dune grasslands

Plant communities with many small annuals and often abundant ephemeral spring bloom, with *Malcolmia* sp, of deep sands and grey dunes of the coasts (Figure 31). Vegetation dominated by terophites with spring phenology growing on sand dunes with good content of nitrogen. It often occurs in complex mosaics covering clearings of perennial dune vegetation (eg. *Ammophila arenaria* formations) (Manuale Italiano di interpretazione degli habitat della Direttiva 92/43 CEE - http://vnr.unipg.it/habitat/index.jsp).

EU Habitat 2270*: Wooded dunes with *Pinus pinea* and/or *P. pinaster*

Coastal dunes covered by Mediterranean and Atlantic thermophilous pines woodlands (Pinus halepensis, P. pinea, P. pinaster), often corresponding to substitution facies of artificial origin or to climax formations of evergreen oak (Quercus ilex). On the Italian Adriatic coast, these are mostly plantations and are rarely natural formations, even if they host maquis and evergreen oak in the undergrowth (Figure 31). They generally occupy the inland stable sector of dune systems. Many stations are currently threatened by marine erosion(Manuale Italiano di interpretazione degli habitat della Direttiva 92/43 CEE - http://vnr.unipg.it/habitat/index.jsp).

Coastal dune mosaics, as those occurring in Torre Cerrano Marine Protected area could be considered well preserved if all the natural habitats (i.e. embryodunes, main fore dunes, transition and fixed back dunes) are present and placed in their natural order (Carboni et al. 2009). The persistence over time of a natural arrangement of coastal dune habitats is fundamental in order to guarantee the ecological functions of the entire coastal dune mosaic. For instance, the sequence of dune plant communities has been found to be directly related with the slope and the aspect of sand dunes and therefore with their stabilizing function (Acosta & Ercole 2015).

At this light, restoration actions aimed at preserving or repairing coastal dune zonation are essential to assure dune functioning over time.

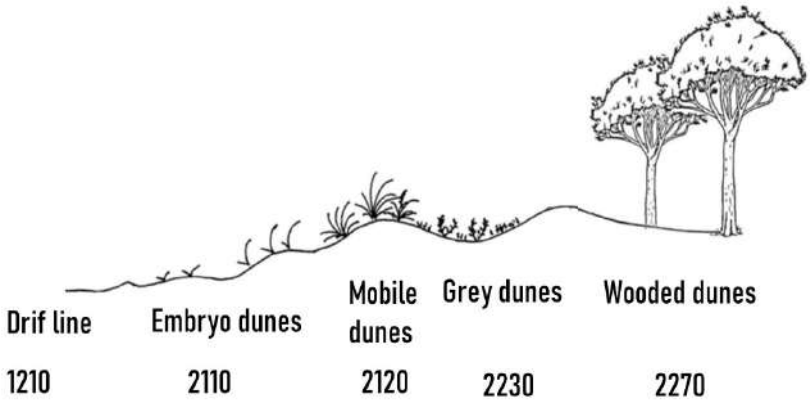

Figure 28. A schematic profile describing the typical Mediterranean coastal dune vegetation zonation present in Torre Cerrano Marine Protected Area and the analyzed EU habitat types codes (Habitats

Directive - HD-92/43/EEC). A description of the habitats and relative photos are reported in the main text.

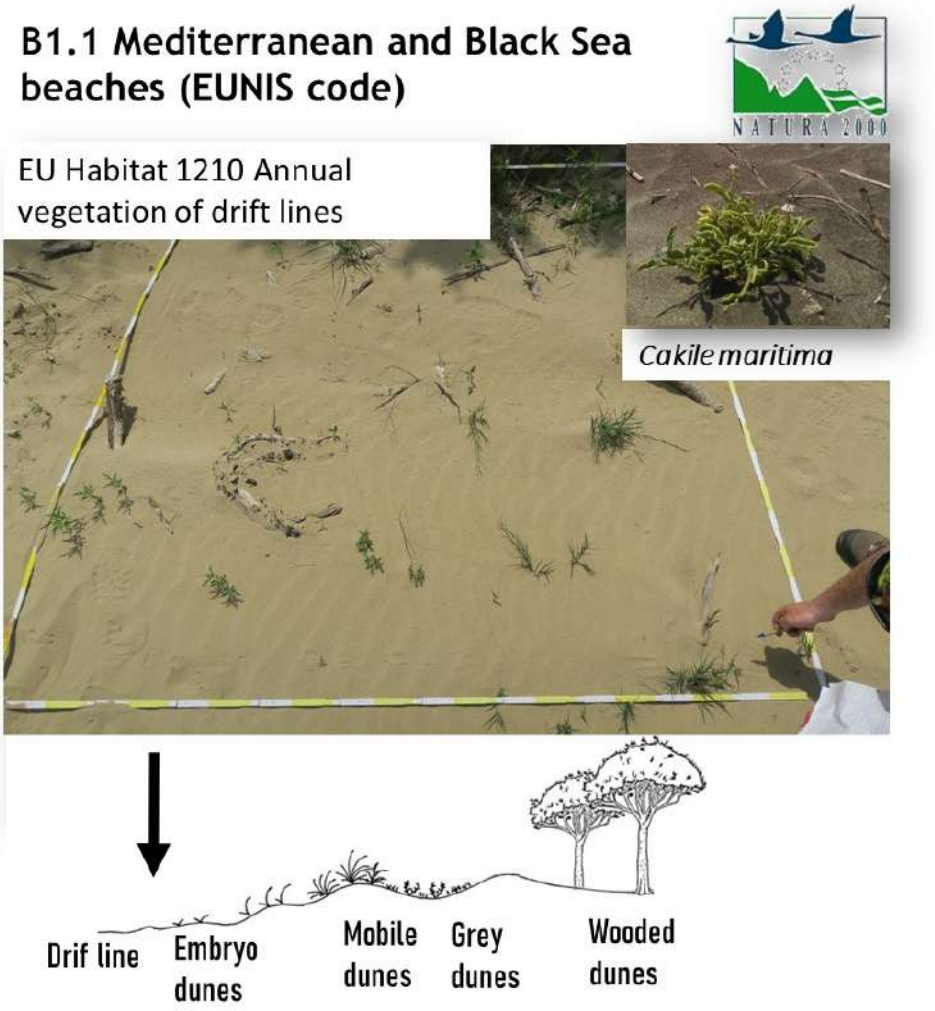

Figure 29: Pictures of Annual vegetation of drift lines (EU Habitat 1210) along with the position of the habitat in the coastal dune zonation present in the Torre Cerrano Marine Protected Area (Pilot area 10)

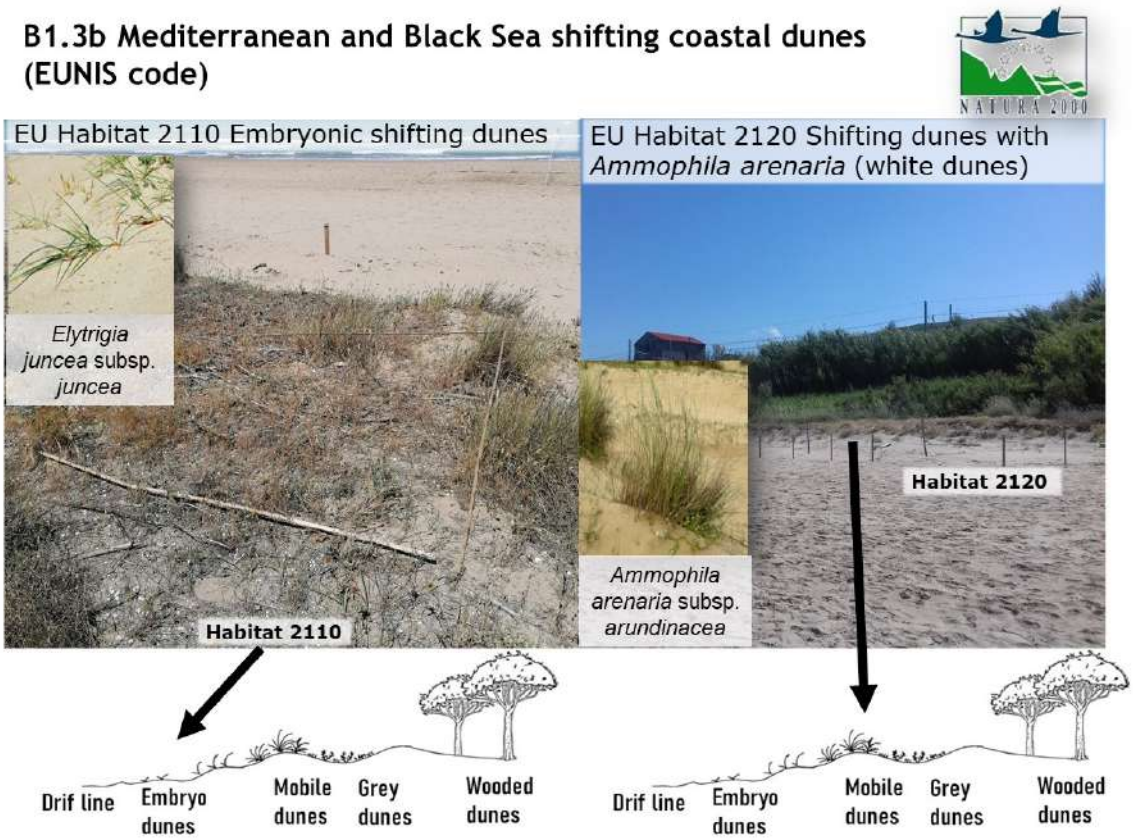

Figure 30: Pictures of Embryonic shifting dunes (EU Habitat 2110, in the left) and Shifting dunes along the shoreline with *Ammophila arenaria* (white dunes; EU Habitat 2120, in the right) along with their position in the coastal dune zonation present in the Torre Cerrano Marine Protected Area (Pilot area 10)

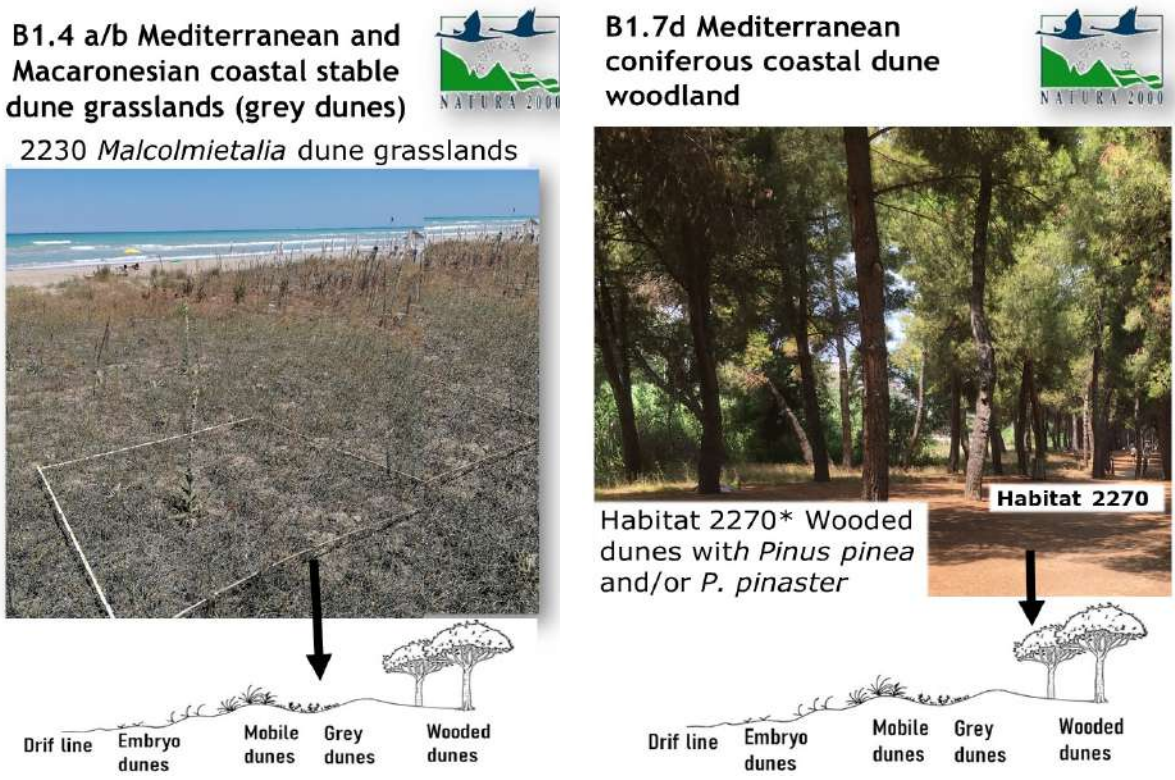

Figure 31: Pictures of Malcolmietalia dune grasslands (EU Habitat 2230) and Wooded dunes with Pinus pinea and/or P. pinaster (EU Habitat 2270* of priority conservation concern in Europe) along with their position of the habitat in the coastal dune zonation present in the Torre Cerrano Marine Protected Area (Pilot area 10)

References

Acosta, A.; Blasi, C.; Carranza, M.L.; Ricotta, C.; Stanisci, A. Quantifying ecological mosaic connectivity and with a new topoecological index. Phytocoenologia 2003, 33, 623–663.

Acosta A.T.R. & Ercole S. (Eds), 2015. Gli habitat delle coste sabbiose italiane: ecologia e problematiche di conservazione. ISPRA, Serie Rapporti, 215/2015

Adam P. 1990. Saltmarsh ecology. Cambridge: Cambridge University Press.

Ahrens, R. N. M.; Walters, C. J.; Christensen, V. 2012. Foraging arena theory: Foraging arena theory. Fish and Fisheries 13, 41–59. doi:10.1111/j.1467-2979.2011.00432.x.

Angelini P., Casella L., Grignetti A., Genovesi P. (ed.), 2016. Manuali per il monitoraggio di specie e habitat di interesse comunitario (Direttiva 92/43/CEE) in Italia: habitat. ISPRA, Serie Manuali e linee guida, 142/2016.

Angelini P., Casella L., Grignetti A., Genovesi P. (ed.), 2016. Manuali per il monitoraggio di specie e habitat di interesse comunitario (Direttiva 92/43/CEE) in Italia: habitat. ISPRA, Serie Manuali e linee guida, 142/2016.

Andreoli, E.; Boscolo, F.; Carlin, A.; Curiel, D.; Gordini, E.; Mizzan, L.; … Zanetto, M. 2010. Side Scan Sonar mosaics of selected northern Adriatic mesophotic biogenic reefs off Venice (GeoTIFF image). Zenodo. http://doi.org/10.5281/zenodo.4608083

Aucelli P.P.C., Iannantuono E., Rosskopf C. M., 2008, Evoluzione e dinamica della costa molisana con particolare riguardo all'equilibrio e alla salvaguardia delle dune, in Mastantuono A. (ed.) Lontano dal Paradiso: Le Dune del Molise, Il Melograno.

Bellafiore, D., Umgiesser, G., 2010. Hydrodynamic coastal processes in the north Adriatic investigated with a 3D finite element model, Ocean Dynam., 60, 255–273.

Beatrici, D.; Braico, P.; Cappelletto, M.;Gallo, E.; Mazari Villanova, L.; Moretti, P.F.;. 2011. "Marine Climate Archives and Geochemical Proxies : A Review and Future Investigations on the Mediterranean Sea National Research Council of Italy Department of Earth and Environment Marine Research at CNR," no. January.

Bellafiore, D., Mc Kiver, W., Ferrarin, C., Umgiesser, G., 2018. The importance of modeling nonhydrostatic processes for dense water reproduction in the southern Adriatic Sea. Ocean Model. 125, 22–28. doi:10.1016/j.ocemod.2018.03.001

Bignami, F., S. Marullo, R. Santoleri, and M. E. Schiano, 1995: Longwave radiation budget in the mediterranean sea. J. Geophys. Res, 100 (C2), 2501–2514, doi:10.1029/94JC02496.

Biondi E., Blasi C., Burrascano S., Casavecchia S., Copiz R., Del Vico E., Galdenzi D., Gigante D., Lasen C., Spampinato G., Venanzoni R., Zivkovic L., 2009, Italian interpretation manual of the 92/43/EEC directive habitats. Ministero dell'Ambiente e della Tutela del Territorio e del Mare, Roma. [online] URL: http://vnr.unipg.it/habitat

Brigolin, D.; Dal Maschio, G.; Rampazzo, F.; Giani, M.; Pastres, R. 2009. "An Individual-Based Population Dynamic Model for Estimating Biomass Yield and Nutrient Fluxes through an off-Shore Mussel (Mytilus Galloprovincialis) Farm." Estuarine, Coastal and Shelf Science 82 (3): 365–76. https://doi.org/10.1016/j.ecss.2009.01.029.

Burchard, H. & Petersen, O., 1999. Models of turbulence in the marine environment—a comparative study of two equation turbulence models. J. Mar. Sys. 21, 29–53

Carboni, M., Carranza, M. L., & Acosta, A. T. (2009). Assessing conservation status on coastal dunes: a multiscale approach. Landscape and Urban Planning, 91(1),17e25

Carrere L., F. Lyard, M. Cancet, A. Guillot, N. Picot, (2016). FES 2014, a new tidal model – Validation results and perspectives for improvements, presentation to ESA Living Planet Conference, Prague.

Clementi, E., Pistoia, J., Delrosso, D., Mattia, G., Fratianni, C., Storto, A., Ciliberti, S., Lemieux, B., Fenu, E., Simoncelli, S., Drudi, M., Grandi, A., Padeletti, D., Di Pietro, P., Pinardi, N., (2017a). A 1/24 degree resolution Mediterranean analysis and forecast modelling system for the Copernicus Marine Environment Monitoring Service. Extended abstract to the 8th EuroGOOS Conference, Bergen.

Clementi, E., Oddo, P., Drudi, M., Pinardi, N., Korres, G., Grandi A., (2017b). Coupling hydrodynamic and wave models: first step and sensitivity experiments in the Mediterranean Sea. Ocean Dynamics. doi: https://doi.org/10.1007/s10236-017-1087-7.

Clementi, E., Aydogdu, A., Goglio, A. C., Pistoia, J., Escudier, R., Drudi, M., Grandi, A., Mariani, A., Lyubartsev, V., Lecci, R., Cretí, S., Coppini, G., Masina, S., & Pinardi, N. (2021). Mediterranean Sea Analysis and Forecast (CMEMS MED-Currents, EAS6 system) (Version 1) [Data set]. Copernicus Monitoring Environment Marine Service (CMEMS). https://doi.org/10.25423/CMCC/MEDSEA_ANALYSISFORECAST_PHY_006_013_EAS6

CMEMS Copernicus Marine Services https://marine.copernicus.eu/

Christensen, V.; Coll, M.; Steenbeek, J.; Buszowski, J.; Chagaris, D.; Walters, C. J. 2014. Representing variable habitat quality in a spatial food web model. Ecosystems 17, 1397–1412. doi: 10.1007/s10021-014-9803-3

CORILA. 2018. Monitoraggio dei banchi di Chamelea gallina: rapporto finale, versione 1.0.

Cutini M., Acosta A.T.R, Molina J. 2010b. Coastal salt-marsh zonation in Tyrrhenian central Italy and its relationship with other Mediterranean wetlands. Plant Biosystems, 144: 1 — 11

Cutini M., Agostinelli E., Acosta A.T.R. & Molina J.A., 2010a. Coastal salt-marsh zonation in Tyrrhenian central Italy and its relationship with other Mediterranean wetlands. Società Botanica Italiana DOI: 10.1080/11263500903178117

Deil U. 2000. Halophytic vegetation along the Arabian coast: Azonal or linked to climatic zones? Phytocoenologia 30(3–4): 591–611.

Dobricic S., and N. Pinardi (2008). An oceanographic three-dimensional variational data ssimilation scheme. Ocean Modelling, 22 (3-4) 89-105.

Drius, M.; Malavasi, M.; Acosta, A.T.R.; Ricotta, C.; Carranza, M.L. Boundary-based analysis for the assessment of coastal dune landscape integrity over time. Appl. Geogr. 2013, 45, 41–48.

Egbert, G., Erofeeva, S., 2002. Efficient inverse modeling of barotropic ocean tides, J. Atmos. Ocean. Tech., 19, 183–204.

Ferrarin, C., Umgiesser, G., Bajo, M., De Pascalis, F., Ghezzo, M., Bellafiore, D., Mattassi, G., Scroccaro, I., 2010. Hydraulic zonation of the Lagoons of Marano and Grado, Italy. A modelling approach. Estuarine Coastal Shelf Sci. 87, 561–572. doi:10.1016/j.ecss.2010.02.012

Ferrarin, C., Roland, A., Bajo, M., Umgiesser, G., Cucco, A., Davolio, S., Buzzi, A., Malguzzi, P., Drofa, O., 2013. Tide-surge-wave modelling and forecasting in the Mediterranean Sea with focus on the Italian coast, Ocean Model., 61, 38–48.

Ferrarin C, Umgiesser G, Roland A, Bajo M, De Pascalis F, Ghezzo M, Scroccaro I. 2016. Sediment dynamics and budget in a microtidal lagoon - a numerical investigation. Mar Geol. 381:163–174

Ferrarin, C., Bellafiore, D., Sannino, G., Bajo, M., Umgiesser, G., 2018. Tidal dynamics in the inter-connected Mediterranean, Marmara, Black and Azov seas. Prog. Oceanogr. 161, 102–115. doi:10.1016/j.pocean.2018.02.006

Ferrarin C, Maicu F, Umgiesser G., 2017. The effect of lagoons on Adriatic Sea tidal dynamics. Ocean Model., 119:57–71.

Federico, I., Pinardi, N., Coppini, G., Oddo, P., Lecci, R., Mossa, M., 2017. Coastal ocean forecasting with an unstructured grid model in the Southern Adriatic and Northern Ionian seas, Nat. Hazards Earth Syst. Sci., 17, 45–59.

Feola, S.; Carranza, M.L.; Schaminée, J.; Janssen, J.A.M.; Acosta, A.T.R. EU habitats of interest: An insight into Atlantic and Mediterranean beach and foredunes. Biodivers. Conserv. 2011, 20, 1457–1468.

Fortibuoni, T.; Canese, S.; Bortoluzzi, G.; Franceschini, G. and O. Giovanardi. 2020. (a). Bathymetry data (GeoTIFF image format) of the Northern Adriatic Tegnùe di Chioggia site collected in 2014-2015 for the DeFishGear project. IEDA. doi:10.26022/IEDA/329816

Gordini, E. and Ciriaco, S. 2020. Bathymetry data (GeoTIFF grid format) of the Northern-most Adriatic area: Interreg Ita-Slo 2007-2013 TRECORALA Project. IEDA. doi:10.26022/IEDA/329903

Gunther, H., Hasselmann, H., Janssen, P.A.E.M., (1993). The WAM model cycle 4, DKRZ report n. 4.

Hasselmann, K. (1974). On the characterization of ocean waves due to white capping, Boundary-Layer Meteorology, 6, 107-127.

Hasselmann, S., and Hasselmann, K. (1985). Computations and parameterizations of the nonlinear energy transfer in a gravity wave spectrum. Part I: A new method for efficient computations of the exact nonlinear transfer integral, J. Phys. Ocean., 15, 1369-1377.

Hasselmann, S., Hasselmann, K., Allender, J.H., Barnett, T.P., (1985). Computations and parameterizations of the nonlinear energy transfer in a gravity wave spectrum. Part II: Parameterizations of the nonlinear energy transfer for application in wave models, J. Phys. Ocean., 15, 1378-1391.

Janssen, P.A.E.M. (1989). Wave induced stress and the drag of air flow over sea wave, J. Phys. Ocean., 19, 745-754.

Janssen, P.A.E.M. (1991). Quasi-Linear theory of wind wave generation applied to wave forecasting, J. Phys. Ocean., 21, 1631-1642.

Jerlov N.G., Optical Oceanography, page 194. Elsevier, 1968.

Kara, B. A., Wallcraft, A. J., Hurlburt, H. E., 2007. A Correction for Land Contamination of Atmospheric Variables near Land–Sea Boundaries, J. Phys. Oceanogr., 37, 803–818.

Killworth PD (2006) Time interpolation of forcing fields in ocean models. J Phys Oceanogr 26:136–143

Komen, G.J., Hasselmann, S., Hasselmann, K., (1984). On the existence of a fully developed windsea spectrum, J. Phys. Ocean., 14, 1271-1285.

Kondo, J. 1975. Air-sea bulk transfer coef- ficients in diabatic conditions. Boundary- Layer Meteorol., 9: 91-112.

Iannantuono E., Rosskopf C.M., Stanisci A., Aucelli P.P.C., 2004, Effetti della dinamica costiera sull'evoluzione dei sistemi dunali presenti lungo la costa molisana (Italia meridionale), Atti dei Convegni dei Lincei, 205, pp. 321-332

Libralato, S., Caccin, A., and Pranovi, F. 2015. "Modeling Species Invasions Using Thermal and Trophic Niche Dynamics under Climate Change." Frontiers in Marine Science 2 (MAY). https://doi.org/10.3389/fmars.2015.00029.

Lynch, D.R and W.G. Gray (1979). A wave equation model for finite element tidal computations. In: Computers & fluids 7.3, pp. 207–228.

Madec, Gurvan and the NEMO team, (2016). NEMO ocean engine: version 3.6 stable. Note du Pole de modelisation, Institut Pierre-Simon Laplace N 27. ISSN No 1288-1619. https://www.nemo-ocean.eu/wp-content/uploads/NEMO_book.pdf

Maderich V., Ilyin Y., Lemeshko E., 2015. Seasonal and interannual variability of the water exchange in the Turkish Straits System estimated by modelling. Mediterranean Marine Science, [S.l.], v. 16, n. 2, p. 444-459, ISSN 1791-6763, doi:http://dx.doi.org/10.12681/mms.1103.

Madricardo, F., Foglini, F., Kruss, A., Ferrarin, C., Pizzeghello, N.M., Murri, C., Rossi, M., Bajo, M., Bellafiore, D., Campiani, E., Fogarin, S., Grande, V., Janowski, L., Keppel, E., Leidi, E., Lorenzetti, G., Maicu, F., Maselli, V., Mercorella, A., Gavazzi, G.M., Minuzzo, T., Pellegrini, C., Petrizzo, A., Prampolini, M., Remia, A., Rizzetto, F., Rovere, M., Sarretta, A., Sigovini, M., Sinapi, L., Umgiesser, G., Trincardi, F., 2017 High-resolution multibeam and hydrodynamic datasets of tidal channels and inlets of the Lagoon of Venice. Sci. Data 4. doi:10.1038/sdata.2017.121

Maicu, F., Alessandri, J., Pinardi, N., Verri, G., Umgiesser, G., Lovo, S., Turolla, S., Paccagnella, T., and Valentini, A.: Down- 70 scaling With an Unstructured Coastal-Ocean Model to the Goro Lagoon and the Po River Delta Branches, Frontiers in Marine Science, 8, 647 781, https://doi.org/10.3389/fmars.2021.647781, 2021.

Manuale Italiano di interpretazione degli habitat della Direttiva 92/43 CEE - http://vnr.unipg.it/habitat/index.jsp

Menegon, S.; Sarretta, A.; Depellegrin, D.; Farella, G.; Venier, C.; Barbanti, A. Tools4MSP: an open source software package to support Maritime Spatial Planning. PeerJ Comput Sci. 2018. 4: e165. doi:10.7717/peerj-cs.165.

Oddo P., N. Pinardi, M. Zavatarelli, 2005. "A numerical study of the interannual variability of the Adriatic Sea (2000-2002)", The Science of the Total Environment, 353, 39-56

Oddo, P., Adani, M., Pinardi, N., Fratianni, C., Tonani, M., Pettenuzzo, D., (2009). A Nested Atlantic-Mediterranean Sea General Circulation Model for Operational Forecasting. Ocean Sci. Discuss., 6, 1093-1127.

Oddo, P., Bonaduce, A., Pinardi, N., Guarnieri, A., (2014) Sensitivity of the Mediterranean sea level to atmospheric pressure and free surface elevation numerical formulation in NEMO. Geosci. Model Dev., 7, 3001–3015.

Pacanowsky, R.C., and Philander S.G.H., (1981) Parameterization of vertical mixing in numerical models of tropical oceans. J Phys Oceanogr 11:1443-1451

Packham JR, Willis AJ. 1997. Ecology of dunes, salt marshes an shingle. London: Chapman & Hall.

Pauly, D.; Christensen, V.; Walters, C. 2000. Ecopath, Ecosim, and Ecospace as tools for evaluating ecosystem impact of fisheries. ICES J. Mar. Sci. 57, 697–706. doi:10.1006/jmsc.2000.0726.

Pettenuzzo, D., Large, W.G., Pinardi, N., (2010) On the corrections of ERA-40 surface flux products consistent with the Mediterranean heat and water budgets and the connection between basin surface total heat flux and NAO. Journal of Geophysical Research 115, C06022, doi:10.1029/2009JC005631

Ponti, M. 2020. (a). 3D wireframe plot of the northern Adriatic mesophotic biogenic reefs. https://zenodo.org/search?page=1&size=20&q=3D%20wireframe%20plot%20tegn%C3%B9a

Ponti, M. 2020. (b). Single-beam bathymetry data (GeoTIFF image format) of selected mesophotic biogenic reefs from the northern Adriatic Sea. IEDA. doi:10.26022/IEDA/329814

Ponti, M. 2020. (c). Single-beam bathymetry data (ESRI ASCII grid format) of selected mesophotic biogenic reefs from the northern Adriatic Sea. IEDA. doi:10.26022/IEDA/329803

Provini A, Crosa G, Marchetti R (1992) Nutrient export from Po and Adige river basins over the last 20 years. Sci Total Environ Suppl:291–313

Reed, R. K. 1977. On estimating insolation over the ocean. J. Phys. Oceanogr., 17: 854- 871.

Russo, Elisabetta, 2020. Tesi di Dottorato in Scienze Ambientali: “Spatial and Temporal Dynamics of Trawl Fishing Activities in the Northern and Central Adriatic Sea (GSA 17) Analysed by Using Automatic Identification System (AIS) Data.”

Simoncelli, S., Pinardi, N., Oddo, P., Mariano, A. J., Montanari, G., Rinaldi, A., and Deserti, M.: Coastal Rapid Environmental As- sessment in the Northern Adriatic Sea, Dynam. Atmos. Oceans, 52, 250–283, 2011.

Smagorinsky, J., 1963. General circulation experiments with the primitive equations. The basic experiment. Monthly Weather Review 91,99–152.

Stanisci A., Carranza M.L., 2008, Lo stato di conservazione del litorale molisano, in Marchetti M., Marino D., Cannata G. (cur.), Relazione sullo stato dell'ambiente della regione Molise, Università degli Studi del Molise Campobasso, pp. 95-96.

Storto, A., Masina, S., Navarra, A., (2015). Evaluation of the CMCC eddy-permitting global ocean physical reanalysis system (C-GLORS, 1982-2012) and its assimilation components. Quarterly Journal of the Royal Meteorological Society, 142, 738–758, doi: 10.1002/qj.2673.

Tolman H.L. (2009). User Manual and system documentation of WAVEWATCH III version 3.14. NOAA/NWS/NCEP/MMAB Technical Note 276, 194 pp + Appendices.

Tolman H.L. (2002). Validation of WAVEWATCH III version 1.15 for a global domain.NOAA / NWS / NCEP / OMB Technical Note 213, 33 pp.

Tonani, M., Balmaseda, M., Bertino, L., Blockley, E., Brassington, G., Davidson, F., Drillet, Y., Hogan, P., Kuragano, T., Lee, T., Mehra, A., Paranathara, F., Tanajura, CAS, Wang, H., (2015) Status and future of global and regional ocean prediction systems. J Operational Oceanography 8:201-220, doi:10.1080/1755876X.2015.1049892.

Tonani, M., Pinardi, N., Dobricic, S., Pujol, I., Fratianni, C., (2008). A high-resolution free-surface model of the Mediterranean Sea. Ocean Sci., 4, 1-14.

Umgiesser, G., Melaku Canu, D., Cucco, A., Solidoro, C., 2004. A finite element model for the Venice Lagoon. Development, set up, calibration and validation. J. Mar. Syst. 51, 123–145. doi: 101016/j.jmarsys.2004.05.009

Umgiesser G, Ferrarin C, Cucco A, De Pascalis F, Bellafiore D, Ghezzo M, Bajo M. 2014. Comparative hydrodynamics of 10 Mediterranean lagoons by means of numerical modeling. J Geophys Res Oceans. 119(4):2212–2226

Walters, C. .1999. Ecospace: Prediction of Mesoscale Spatial Patterns in Trophic Relationships of Exploited Ecosystems, with Emphasis on the Impacts of Marine Protected Areas. Ecosystems 2, 539–554. doi:10.1007/s100219900101.

WRF ARPA FVG http://www.arpa.fvg.it/cms/tema/crma/modelli/modello_wrf.html

WRF ARPA FVG Forecats http://www.arpaweb.fvg.it/fcm/gmapsmt.asp

WRF ARPA FVG hindacast http://www.arpa.fvg.it/export/sites/default/tema/crma/pubblicazioni/docs_pubblicazioni/2019gen05_arpafvg_crma_nausica_interim_rap2019_01.pdf